APPLIED COMPUTER SCIENCE

The Journal is a peer-reviewed, international, multidisciplinary journal covering a broad spectrum of topics of computer application in production engineering, technology, management and economy.

The main purpose of Applied Computer Science is to publish the results of cutting-edge research advancing the concepts, theories and implementation of novel solutions in computer technology. Papers presenting original research results related to applications of computer technology in production engineering, management, economy and technology are welcomed.

We welcome original papers written in English. The Journal also publishes technical briefs, discussions of previously published papers, book reviews, and editorials. Especially we welcome papers which deals with the problem of computer applications in such areas as:

- manufacturing,
- engineering,
- technology,
- designing,
- organization,
- management,
- economics,
- innovations,
- competitiveness,
- quality and costs.

The Journal is published quarterly and is indexed in: BazTech, Cabell's Directory, CNKI Scholar (China National Knowledge Infrastucture), ERIH PLUS, Index Copernicus, J-Gate, Google Scholar, TEMA Technik und Management.

Letters to the Editor-in-Chief or Editorial Secretary are highly encouraged.

CONTENTS

Lucian LUPŞA-TĂTARU [0000-0002-3320-9850]*

IMPLEMENTING THE FADE-IN AUDIO EFFECT FOR REAL-TIME COMPUTING

Abstract

Audio fading is performed in order to smoothly modify over time the level of an audio signal. In particular, the fade-in audio effect designates a gradually increase in the audio volume, starting from silence. In practice, audio fading is mostly carried out within audio editors i.e. in off-line mode by employing various transcendental functions to enforce the fade profile. Taking into account the increasing demand for interactive media services requiring real-time audio processing, the present approach advances an effective method of constructing the audio fade-in shape with a view to real-time computing. The paper encompasses plain and straightforward implementations in pure JavaScript, prepared precisely to validate the method of audio volume processing proposed here.

1. INTRODUCTION

The nature of interactive computing, which is essential for a two-way effective communication between machine and user, implies fast computing and employment of event-driven programming style. On the other hand, with the recent release of the fifth version (HTML5) of HTML standard, which natively allows the control of multimedia content, complex web applications have arisen to complement the traditional native applications on the various low-powered devices. Also, the functionality of the new set of rules characteristic of HTML5 appears to be very convenient to enhance by event-driven programming carried out in JavaScript (Devlin, 2012; Jacobs, Jaffe & Le Hegaret, 2012; Powers, 2011; *HTML 5.2. W3C Recommendation*, 2017).

---

* Transilvania University of Braşov, Faculty of Electrical Engineering and Computer Science, Department of Electrical Engineering and Applied Physics, Bd. Eroilor No. 29, Braşov, RO-500036, Romania, lupsa@programmer.net, lucian.lupsa@unitbv.ro

In this context, having in view that designing of media development software, simulation software as well as entertainment applications often asks for real-time/fast audio processing, the present investigation puts forward an effective solution for constructing the profile of the fade-in audio effect. Although widely used in order to receive a smooth lead in to an audio content, the fade-in sound effect is usually applied within audio editors that is in off-line mode, by employing linear and transcendental functions to impose the time-related evolution of the audio volume, starting from a level of 0 (silence) (Case, 2007; Jackson, 2015; Langford, 2014; Reiss & McPherson, 2015).

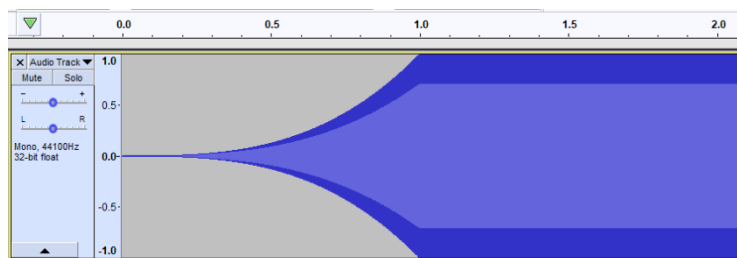**Fig. 1. An exponential fade-in audio effect, received in Audacity editor for the final audio level of 1 and the fade length of 1 s**
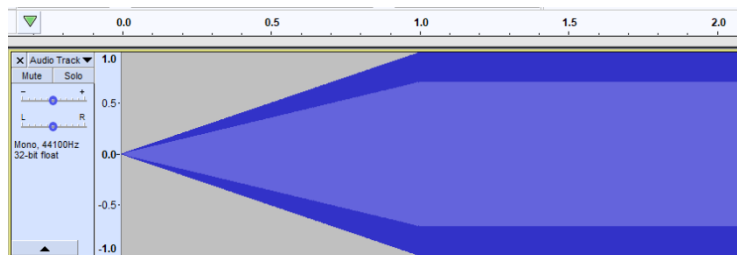

Fig. 2. A linear fade-in audio effect, received in Audacity editor for the final audio level of 1 and the fade length of 1 s
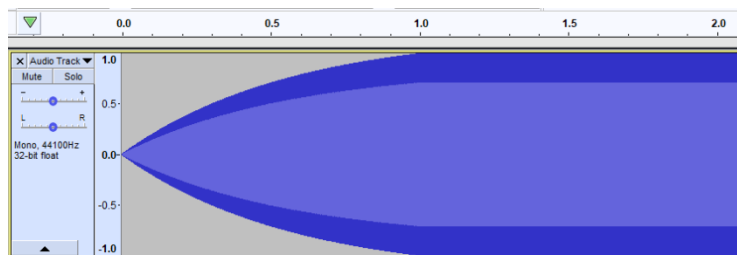

Fig. 3. A logarithmic fade-in audio effect, received in Audacity editor for the final audio level of 1 and the fade length of 1 s

Fig. 1, Fig. 2 and Fig. 3 highlight a set of 1 s length fade-ins of exponential, linear, and logarithmic curve shape, carried out in Audacity editor (Jackson, 2015; Schroder, 2011). It has to be emphasized that both fade-in length and shape should be correlated with the appropriate music genre (Corey, 2017; Panagakis, Kotropoulos & Arce, 2014; Potter, 2002).

By adopting the exponential fade-in, depicted in Fig. 1, one receives an extremely smooth transition from silence, characterized by a low instantaneous rate of change of audio level in the beginning of fading-in. As the opposite of the exponential fade-in shape, the fade-in of logarithmic type, illustrated in Fig. 3, determines a quick increase of the audio volume in the beginning of the fade effect, followed by a decrease in the rate of change of audio volume towards the end of fading-in. Hence, a logarithmic fade-in brings a soft increase in the audio level within the ending region of the effect. On the other hand, as Fig. 2 indicates, the linear fade-in effect is performed at a constant rate of change of audio level and, obviously, in this case, any attempt of smoothing the transition from silence would lead to an increasing of the fade-in length (Case, 2007; Langford, 2014; Reiss & McPherson, 2015).

With a view to real-time computing, one has to consider that the instant of fade-in initiation is associated with an event occurrence, and that the valuation of the outputs of transcendental functions, suitable for shaping the fade-in profile in the off-line mode, comes to be very time consuming.

2. CUSTOMIZING THE FADE-IN PROFILE

To improve the computational capabilities with the purpose of real-time processing, we consider that the evolution of audio volume during fading-in is given here by the output of the following rational function of time variable:

$$\begin{cases} v(t) = \frac{\alpha t^k}{t+\beta}, & t \in [0, t_f] \\ k \in \{1,2,3\} \end{cases} \tag{1}$$

where: t_f – designates the fade-in length.

In contrast to valuating the outputs of different transcendental functions, which proved to be suitable for customizing the audio fade-in shape in the off-line mode, e.g. within various audio editors, the implementation of (1) does not require for auxiliary functions or methods to be called, regardless of the adopted programming language. It has to be noticed that the approach corresponding precisely to $k = 2$ in (1) has already been considered in order to construct fade-ins that act, in real-time, similar to the fade-in audio effect of exponential curve shape (Lupsa-Tataru, 2017). Nevertheless, it will be shown that the fade-ins

received by computing the more comprehensive expression (1) can act either as the fade-in audio effect of exponential type or as the fade-in audio effect of logarithmic curve shape.

With the time-related audio level provided by (1), the instantaneous rate of change of the audio volume during fading-in comes to be:

$$
\begin{aligned}
v'(t) &\equiv \frac{dv}{dt} = \frac{d}{dt}\left(\frac{\alpha t^k}{t+\beta}\right) \\
&= \alpha[(k-1)t + k\beta]\frac{t^{k-1}}{(t+\beta)^2}
\end{aligned}
\tag{2}
$$

Since the fade-in audio effect is represented by a strict increasing in the signal level, it plainly follows that function (1) has to be strictly increasing (Langford, 2014; Reiss & McPherson, 2015). Having in view (2), this implies:

$$
\alpha[(k-1)t + k\beta] > 0.
\tag{3}
$$

On the other hand, if we denote the fade-in halfway point i.e. the fade-in midpoint by means of variable

$$
t_h = t_f/2,
\tag{4}
$$

then, in order to receive a strict increasing in the level of the audio signal, starting from silence, the following conditions come to be essential:

$$
v(t_h) = v_h = \rho_h v_f,
\tag{5}
$$

$$
v(t_f) = v_f,
\tag{6}
$$

wherein, we have

$$
v(0) = 0 < v_h < v_f,
\tag{7}
$$

$$
\rho_h = v_h/v_f.
\tag{8}
$$

Within relations (5)–(8), variable v_h indicates the imposed audio level at the fade-in midpoint (4) whilst variable v_f designates the final volume i.e. the audio level to be reached at the end of fading-in. In this context, taking now into account merely (7) and (8), one obtains

$$
0 < \rho_h < 1.
\tag{9}
$$

Having in view that the function employed to construct the fade-in profile is given by (1), conditions (5) and (6) lead to the following system of algebraic equations:

$$
\begin{cases}
\dfrac{\alpha t_f^k}{t_f + 2\beta} = 2^{k-1} \rho_h v_f \\[2ex]
\dfrac{\alpha t_f^k}{t_f + \beta} = v_f
\end{cases}.
\tag{10}
$$

One perceives that (10) is linear with respect to the encompassed coefficients α and β. More precisely, one straightforwardly obtains that (10) is equivalent to:

$$
\begin{cases}
t_f^k \cdot \alpha - 2^k \rho_h v_f \cdot \beta = 2^{k-1} \rho_h t_f v_f \\
t_f^k \cdot \alpha - v_f \cdot \beta = t_f v_f
\end{cases}.
\tag{11}
$$

For a specific value of k in (1), the solution of (11) yields the coefficients of (1) in terms of fade length t_f, the final volume v_f, and quantity (8) that depends on the imposed audio level at the fade-in halfway point (4). One receives:

$$
\alpha = \frac{2^{k-1} \rho_h v_f}{2^k \rho_h - 1} \cdot \frac{1}{t_f^{k-1}},
\tag{12}
$$

$$
\beta = \frac{1 - 2^{k-1} \rho_h}{2^k \rho_h - 1} t_f .
\tag{13}
$$

In order to fulfill condition (3) of enforcing a positive rate of change of the audio level, we plainly consider $\alpha > 0$ and $\beta > 0$, respectively. In this context, by inspecting expressions (12) and (13) of the two coefficients, the following conditions arise:

$$
\begin{cases}
2^k \rho_h - 1 > 0 \\
1 - 2^{k-1} \rho_h > 0
\end{cases}
\tag{14}
$$

or, what is just equivalent

$$
\frac{1}{2^k} < \rho_h < \frac{1}{2^{k-1}} .
\tag{15}
$$

Thus, based on (12), (13) and (15), one finds that the time-related expression of the algebraic fraction (1), which shapes the audio fade-in profile, incorporates the parameters:

$$k = \begin{cases} 3, & 1/8 < \rho_h < 1/4 \\ 2, & 1/4 < \rho_h < 1/2, \\ 1, & 1/2 < \rho_h < 1 \end{cases} \tag{16}$$

$$\alpha = \alpha(\rho_h) = \begin{cases} \dfrac{4\rho_h v_f}{8\rho_h - 1}\dfrac{1}{t_f^2}, & 1/8 < \rho_h < 1/4 \\[2mm] \dfrac{2\rho_h v_f}{4\rho_h - 1}\dfrac{1}{t_f}, & 1/4 < \rho_h < 1/2, \\[2mm] \dfrac{\rho_h v_f}{2\rho_h - 1}, & 1/2 < \rho_h < 1 \end{cases} \tag{17}$$

$$\beta = \beta(\rho_h) = \begin{cases} \dfrac{1 - 4\rho_h}{8\rho_h - 1}t_f, & 1/8 < \rho_h < 1/4 \\[2mm] \dfrac{1 - 2\rho_h}{4\rho_h - 1}t_f, & 1/4 < \rho_h < 1/2, \\[2mm] \dfrac{1 - \rho_h}{2\rho_h - 1}t_f, & 1/2 < \rho_h < 1 \end{cases} \tag{18}$$

wherein one observes that the value of k out of the set {1,2,3} as well as the appropriate expressions of the coefficients are decided by the value of quantity (8) that is the ratio between the imposed audio level at the fade-in midpoint and the final audio level.

Since both coefficients (17) and (18), interfering in (1), are positive and, also, $k \in \{1,2,3\}$, it follows that condition (3) of receiving a gradual increasing in the level of the audio content is now fulfilled. Hence, with (16)–(18), one obtains:

$$v'(t) \equiv \frac{dv}{dt} > 0, \quad t > 0 \tag{19}$$

and, having in view (2),

$$v'(0) \equiv \frac{dv}{dt}\bigg|_{t=0} = \begin{cases} 0, & 1/8 < \rho_h < 1/4 \\ 0, & 1/4 < \rho_h < 1/2. \\ \alpha/\beta, & 1/2 < \rho_h < 1 \end{cases} \tag{20}$$

Considering (1), (2) and (16), then, for $1/8 < \rho_h < 1/4$, one explicitly gets the appropriate expression of the rational function shaping the fade-in profile along with the appropriate expression of the instantaneous rate of change of the audio volume during fading-in i.e.

$$v(t) = \frac{\alpha t^3}{t + \beta}, \quad t \in [0, t_f], \tag{21}$$

$$v'(t) \equiv \frac{dv}{dt} = \alpha(2t + 3\beta)\frac{t^2}{(t + \beta)^2} > 0, \quad t > 0. \tag{22}$$

Similarly, for $1/4 < \rho_h < 1/2$, one explicitly receives

$$v(t) = \frac{\alpha t^2}{t + \beta}, \quad t \in [0, t_f], \tag{23}$$

$$v'(t) \equiv \frac{dv}{dt} = \alpha(t + 2\beta)\frac{t}{(t + \beta)^2} > 0, \quad t > 0. \tag{24}$$

while for $1/2 < \rho_h < 1$, the rational function (1), modelling the fade-in profile, and the corresponding rate of change of audio level, yielded by (2), come to be

$$v(t) = \frac{\alpha t}{t + \beta}, \quad t \in [0, t_f], \tag{25}$$

$$v'(t) \equiv \frac{dv}{dt} = \frac{\alpha\beta}{(t + \beta)^2} > 0, \quad t \in [0, t_f]. \tag{26}$$

3. THE FADE-IN CURVES

Based on (1), (16)–(18), in Fig. 4, Fig. 5, and Fig. 6, we have illustrated the fade-in profiles for fade length $t_f = 0.5$ s, $t_f = 1$ s and $t_f = 2$ s, respectively, with quantity (8) selected as parameter. Since the validation of the suggested technique of real-time performing the fade-in audio effect is accomplished here by means of plain JavaScript implementations, we have considered that the final volume i.e. the volume to be reached at the end of fading-in has the value of 1 that is the default and, also, the highest volume adopted in HTML5 (Devlin, 2012; Powers, 2011; *HTML 5.2. W3C Recommendation*, 2017). In this context, quantity (8) represents just the audio level imposed at the fades midpoint (4) i.e. $t_h = 0.25$ s for Fig. 4, $t_h = 0.5$ s for Fig. 5 and $t_h = 1$ s for Fig. 6, respectively.

One observes that the fade-ins of Fig. 4, Fig. 5 and Fig. 6, respectively, received for $\rho_h = 0.15$ and $\rho_h = 0.3$, will act similar to the fade-in audio effect of exponential curve shape i.e. the audio level will increase smoothly till the midpoint, starting from an initial rate of change of zero, as (20) indicates, and, then, it will slope upwards with an increasing rate of change, according to (21)

11

and (23), respectively. At the opposite side, the fade-ins corresponding to $\rho_h = 0.7$ and $\rho_h = 0.85$ will act similar to the fade-in of logarithmic shape i.e. the audio level will go up quickly till the halfway point, and, subsequently, it will increase slowly towards the end of fading-in, in accordance with the time-related evolution enforced by (25).
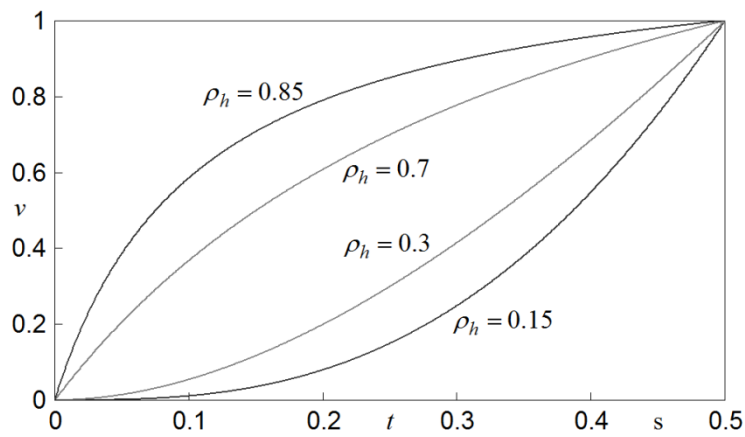

Fig. 4. Fade-in curves for the fade length of 0.5 s and the final volume of 1 (the default value in HTML5)
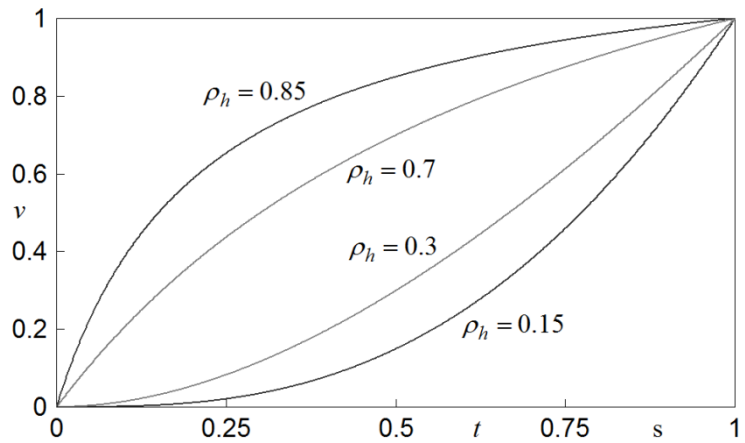

Fig. 5. Fade-in curves for the fade length of 1 s and the final volume of 1 (the default value in HTML5)
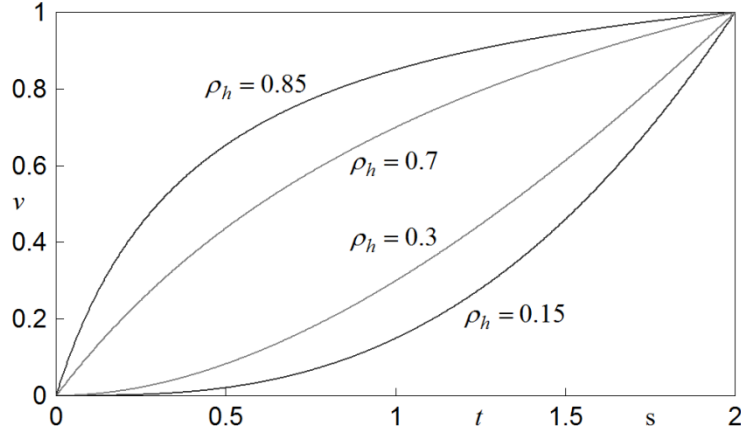
12

**Fig. 6. Fade-in curves for the fade length of 2 s and the final volume of 1
(the default value in HTML5)**

Thus, all the three figures, plotted for $\rho_h \in \{0.15, 0.3, 0.7, 0.85\}$, do highlight that the received profiles are crucially decided by the value of quantity (8), regardless of the fade-in length, what validates the generality of function (1), employed for fade shaping.

4. JAVASCRIPT IMPLEMENTATIONS

In order to verify the suggested method of fade-in profile customizing for the suitability with real-time computing, we have developed straightforward implementations in plain ("vanilla") JavaScript, with the discretization being achieved by employing the "setInterval()" method of the "window" object. For the sake of simplicity, the two applications advanced in the paper have been optimized so that the only intervention of the user consists in providing the appropriate audio content (sample) upon which the fade-in effect has to be applied.

The first application has been implemented by taking into account the more complex relations (16)–(18). Therefore, although we have set the value of 0.15 for quantity (8) in order to receive a 2 s audio fade-in that acts similar to the fade-in effect of exponential curve shape (see Fig. 6), a function is incorporated just to compute the parameters of (1) for any value of ratio (8) that is located within the open intervals of representations (16)–(18). One perceives that as a result of linking the "play" media event to the audio element, the fade-in effect is applied, from the beginning of the audio sample, whenever the audio has been started. As aforementioned, the discrete-time processing is accomplished here by means of the "setInterval()" method of the "window" object. More precisely, as the code plainly indicates, once every 50 ms, the current position within the audio

13

content (sample) i.e. the audio object "currentTime" property is passed to a specialized function that returns the output of rational function (1), which, in turn, is used to update the audio object "volume" property. The code of the described application is put forward in what follows right away.

Listing 1. The code of the described application

```
<!DOCTYPE html>
<html>
<head>
<title>Fade-in</title>
</head>
<body>
<script>

var ae;                 // the audio element (object)
var k, alpha, beta;     // parameters of the rational function, shaping
                        // the fade-in
var timerId;            // id value returned by setInterval() method

function compPrm( tF, vF, rhoH ) {
/* computes the parameters of the algebraic fraction (1);
function arguments: fade length, final volume i.e. audio volume to be
reached, ratio (8) between the audio volume at fade-in midpoint and the
final volume */

   var rhoH2 = rhoH + rhoH;
   var rhoH4, rhoH8, auxVar;
           // auxiliary variables
   if ( 0.5 < rhoH && rhoH < 1.0 ) {
      k = 1;
      auxVar = rhoH2 - 1.0;
      alpha = rhoH * vF / auxVar;
           // based on representation (17), for 1/2 < rhoH < 1
      beta = ( 1.0 - rhoH ) * tF / auxVar;
           // based on representation (18), for 1/2 < rhoH < 1
   }
   else if ( 0.25 < rhoH && rhoH < 0.5 ) {
      k = 2;
      rhoH4 = rhoH2 + rhoH2;
      auxVar = rhoH4 - 1.0;
      alpha = rhoH2 * vF / auxVar / tF;
           // based on representation (17), for 1/4 < rhoH < 1/2
      beta = ( 1.0 - rhoH2 ) * tF / auxVar;
           // based on representation (18), for 1/4 < rhoH < 1/2
   }
   else {        // 0.125 < rhoH && rhoH < 0.25 (1/8 < rhoH < 1/4)
      k = 3;
      rhoH4 = rhoH2 + rhoH2; rhoH8 = rhoH4 + rhoH4;
      auxVar = rhoH8 - 1.0;
      alpha = rhoH4 * vF / auxVar / tF / tF;
           // based on representation (17), for 1/8 < rhoH < 1/4
      beta = ( 1.0 - rhoH4 ) * tF / auxVar;
           // based on representation (18), for 1/8 < rhoH < 1/4
   }
}
```

14

```javascript
function v( t ) {
/* returns the output of the rational function shaping the fade-in,
for a given instant of time */
   var newVol = alpha * t / ( t + beta );
           // algebraic fraction (25), corresponding to 1/2 < rhoH < 1
   if ( k == 2 ) { newVol = newVol * t; }
           // algebraic fraction (23), corresponding to 1/4 < rhoH < 1/2
   else if ( k == 3 ) { newVol = newVol * t * t; }
           // algebraic fraction (21), corresponding to 1/8 < rhoH < 1/4
   return newVol;
}

function setVol( vF ) {
/* sets the audio volume during fading-in;
argument: final volume i.e. the audio volume to be reached */
   var timeVar = ae.currentTime;
           // the current position within the audio content, in second
   var currentVol = v( timeVar );
           // calls v( t ), with parameter t receiving the current
           // playback time
   if ( currentVol < vF ) { ae.volume = currentVol; }
   else {
      ae.volume = vF;                      // volume supressing
      window.clearInterval( timerId );    // clears the timer
   }
}

function fadeIn() {
/* performs the audio fading-in by means of
setInterval() method of the window object */
   ae.currentTime = 0.0; ae.volume = 0.0;
      // audio object properties initialization;
      // the fade-in effect is initiated just at the beginning of audio
      // content
   timerId = window.setInterval( setVol, 50, 1.0 );
      // the setInterval() method calls setVol() function once every 50 ms;
      // the setInterval() method passes the value of 1 to parameter vF
}

compPrm( 2.0, 1.0, 0.15 );
           // arguments: fade length of 2 s, final volume of 1, ratio (8)
           // of 0.15
ae = document.createElement( "AUDIO" );
           // creates the audio element (object)
ae.controls = true;        // displays audio controls
ae.src = "sample.mp3";     // indicates an audio/mpeg file; provided by user
ae.addEventListener( "play", fadeIn );
           // associates the play event swith the audio element
document.body.appendChild( ae );
           // appends the created audio element to the document

</script>
</body>
</html>
```

The implementation given next has been reduced to a straightforward and short structure in order to highlight a significant benefit that comes from associating the "play" media event with the audio element (Lupsa-Tataru, 2017).

Listing 2. Reduced structure of developed code

```html
<!DOCTYPE html>
<html>
<head>
<title>Fade-in</title>
</head>
<body>
<script>

var ae;
var alpha, beta;

var refTime;
   // holds the playback position when the audio has started to play

var timerId;

function compPrm( tF, vF, rhoH ) {
   // for the case of 1/8 < rhoH < 1/4 only
   var rhoH4 = rhoH + rhoH; rhoH4 = rhoH4 + rhoH4;
   var rhoH8 = rhoH4 + rhoH4;
   var auxVar = rhoH8 - 1.0;
   alpha = rhoH4 * vF / auxVar / tF / tF;
   beta = ( 1.0 - rhoH4 ) * tF / auxVar;
}
function v( t ) {
   var newVol = alpha * t * t * t / ( t + beta );
   return newVol;
}
function setVol( vF ) {
   var tau = ae.currentTime - refTime;
   var currentVol = v( tau );
   if ( currentVol < vF ) { ae.volume = currentVol; }
   else {
      ae.volume = vF;
      window.clearInterval( timerId );
   }
}
function fadeIn() {
   refTime = ae.currentTime; ae.volume = 0.0;
   timerId = window.setInterval( setVol, 50, 1.0 );
}

compPrm( 2.0, 1.0, 0.15 );
ae = document.createElement( "AUDIO" );
ae.controls = true;
ae.src = "sample.mp3";
ae.addEventListener( "play", fadeIn );
document.body.appendChild( ae );

</script>
</body>
</html>
```

One observes that, although this second implementation has been designed to work merely for the case of $1/8 < \rho_h < 1/4$, it comes with the plus of allowing the initiation of the fade-in effect not only at the beginning of the audio content but also whenever the audio is no more paused. This obviously will smooth the listening experience for long audio contents on audio/video sharing platforms, when the user alternatively accesses the "play" and "pause" standard media controls. To gain benefit, in addition to the first application, we have introduced the "refTime" variable of global scope in order to hold the playback position within the audio content whenever the user accesses the "play" audio control. Hence, the fade-in audio effect is applied here with respect to the current value of "refTime" global variable i.e. according to (21), wherein the following replacement is to be performed

$$t \leftarrow \tau;$$
$$\tau = t - t_{ref}$$

with t_{ref} standing for the value of "refTime" variable of the implementation, which comes now to be the instant of fade-in initiation.

5. CONCLUSIONS

Audio fade-ins are widely used to smooth the transition from silence of audio signals (Case, 2007; Jackson, 2015; Langford, 2014; Reiss & McPherson, 2015; Schroder, 2011). They are usually applied within audio editors, i.e. in off-line mode, by employing different transcendental functions of time variable to impose the evolution of audio level. However, the design of various interactive products, like simulation software and entertainment applications, frequently calls for fast audio processing techniques. By adopting a rational function to enforce the time-related evolution of the audio volume, the present investigation advances an efficient method of constructing the audio fade-in profile, suitable for real-time computing. It is shown that the resulted fade-ins, straightforwardly obtained by valuating the output of the selected rational function for numerous values of the encompassed parameters, can act either as the audio fade-in of exponential type or as the audio fade-in of logarithmic shape.

With the audio content/sample as the preference of the reader, the optimized implementations in pure JavaScript, put forward in the present paper, plainly emphasize the effectiveness of the proposed solution to constructing the audio fade-in profile.

Further developments could be geared towards real-time audio cross-fading techniques, by employing the method of audio fading-in suggested here along with a technique of audio fading-out suitable for fast computing (Lupsa-Tataru, 2018).

REFERENCES

Case, A. U. (2007). *Sound FX: Unlocking the Creative Potential of Recording Studio Effects.* Burlington, MA, USA: Focal Press.

Corey, J. (2017). *Audio Production and Critical Listening: Technical Ear Training.* New York, NY, USA: Routledge.

Devlin, I. (2012). *HTML5 Multimedia: Develop and Design.* Berkeley, CA, USA: Peachpit Press.

Jackson, W. (2015). *Digital Audio Editing Fundamentals: Get started with digital audio development and distribution.* Berkeley, CA, USA: Apress Media. doi:10.1007/978-1-4842-1648-4

Jacobs, I., Jaffe, J., & Le Hegaret, P. (2012). How the open web platform is transforming industry. *IEEE Internet Computing, 16*(6), 82-86. doi:10.1109/MIC.2012.134

Langford, S. (2014). *Digital Audio Editing: Correcting and Enhancing Audio in Pro Tools, Logic Pro, Cubase, and Studio One.* Burlington, MA, USA: Focal Press.

Lupsa-Tataru, L. (2017). Shaping the fade-in audio effect with a view to JavaScript implementation. *Journal of Computations & Modelling, 7*(4), 111−126.

Lupsa-Tataru, L. (2018). Novel technique of customizing the audio fade-out shape. *Applied Computer Science, 14*(3), 5−14. doi:10.23743/acs-2018-17

Panagakis, Y., Kotropoulos, C. L., & Arce, G. R. (2014). Music genre classification via joint sparse low-rank representation of audio features. *IEEE/ACM Transactions on Audio, Speech, and Language Processing, 22*(12), 1905−1917. doi:10.1109/TASLP.2014.2355774

Potter, K. (2002). *Four Musical Minimalists: La Monte Young, Terry Riley, Steve Reich, Philip Glass (Series: Music in the Twentieth Century).* Cambridge, UK: Cambridge University Press.

Powers, S. (2011). *HTML5 Media.* Sebastopol, CA, USA: O'Reilly Media.

Reiss, J. D., & McPherson, A. (2015). *Audio Effects: Theory, Implementation and Application.* Boca Raton, FL, USA: CRC Press.

Schroder, C. (2011). *The Book of Audacity: Record, Edit, Mix, and Master with the Free Audio Editor.* San Francisco, CA, USA: No Starch Press.

WebPlat WG (Web Platform Working Group). (2017). *HTML 5.2. W3C Recommendation.* W3C technical reports index: https://www.w3.org/TR/2017/REC-html52-20171214

Hamid JAN [0000-0003-2065-8515]*, *Amjad ALI**

OPTIMIZATION OF FINGERPRINT SIZE FOR REGISTRATION

Abstract

The propose algorithm finds the optimal reduced size of latent fingerprint. The algorithm accelerates the correlation methods of fingerprint registration. The Algorithm is based on decomposition and reduction of fingerprint to one dimension form by using the adoptive method of empirical modes. We choose the most appropriate internal mode to determine the minimum distance between the extremes of empirical modes. We can estimate how many times the fingerprint in the first step of the comparison can be reduced so as not to lose the accuracy of registration. This algorithm shows best results as compared to conventional fingerprint matching techniques that strongly depends on local features for registration. The algorithm was tested on latent fingerprints using FVC2002, FVC2004 and FVC2006 databases.

1. INTRODUCTION

Identification of a person using fingerprints has been used for many years. Traditionally, the people that act as driving force behind the promotion of fingerprint technologies have become law enforcement agencies and forensic professionals. The use of fingerprints taken at the scene of crime to identify suspects can be a decisive stage in the criminal examination; Figure 1 shows fingerprints taken from crime scene. Massive fingerprint databases have been collected by law enforcement agencies around the world. These large databases

---

* Sarhad University of Science & Information Technology, Landi Akhun Ahmad,
Hayatabad Link, Ring Road, Peshawar 25000, Pakistan, hod.csit@suit.edu.pk

encourage research work to towards development of Identification systems by fingerprints. The latent fingerprints collected from crime scene are noisy, low resolution and contain little information. Matching latent fingerprints is a challenge.

Fig. 1. Latent Finger Print [source: database of Indraprastha Institute of Information Technology]

Many fingerprint matching algorithms are based on a comparison of small fingerprints features known as minutiae (Yager & Amin, 2004). These features are of many types. During the minutiae extraction phase, any errors will extend to the stages of alignment and verification, which are dependent on the quality of minutiae information. Some researcher took interest in matching techniques, not dependent on minutiae, like pixel intensities (Bazen, Verwaaijen, Gerez, Veelenturf & Zwaag, 2000) or filter banks which are based on orientation information (Park, Lee, Smith, Park & Park, 2004).

2. RELATED WORK

In this section, we identify some studies conducted on fingerprint registration. Transformation by Hough for fingerprint registration was proposed (Ratha, Karu, Chen & Jain, 1996). The volume is converted into a discrete set of values of all possible transformations. The rotation and translation to register them is computed for each pair of significant matching minutiae. Proof of this transformation is collected in the parameter space. To select the most likely transformation parameters, the minutiae space is used. The main disadvantage of this method is that it is computationally expensive. However it will work properly, since the performance of method is a very broad search of the parameters volume. This approach is based on minutiae and can be compared with minutiae based registration algorithms.

The main disadvantage of transformation of Hough is its execution time. Several attempts have been made to develop more efficient matching algorithms. A commonly used technique is to provide additional information that leads to leveling and decreasing the number of dependent values (Bazen, Verwaaijen, Gerez, Veelenturf & Zwaag, 2000; Jain, Hong & Bolle, 1997; Park, Lee, Smith, Park & Park, 2004; Ratha, Karu, Chen & Jain, 1996; Yager & Amin, 2004) uses ridge information as an registration help and this approach has been implemented. During the extraction of minutiae, the form of its associated ridge is also stored.

In the case of a possible pair of details, if the corresponding ridges are the same, the minutia pairs are in the same place. Then they are rotated to even the projections. This rule applies to all possible minutiae pairs and alignment, which leads to the most global match.

Structural approaches utilize local fingerprint feature mechanisms to quickly find possible matching items. An algorithm of structural matching proposed by Jiang (Jiang & Yau, 2000) has been developed. The data used in this approach is the distance between fingerprint local features, the relative differences between the radial angles and the directions of minutiae, the types of details and the size of the ridges. This information is used to search for possible curiosities. Then, the registration parameters are calculated to register this match.

The only approach of non-minutiae for registration is based on the alignment of checkpoints. Maes, Vandermeulen & Suetens (2003) define a reference point (or base point) as the point of maximum curvature of concave ridges in the fingerprint. The authors create a way to identify the main points that use the mask to integrate sine components of local orientations. This method was used to determine the position of the reference point. After extracting the control point from each fingerprint, the registration is done by searching for parameters that align them. It should be noted that this includes only translation parameters (no rotation).

3. METHODOLOGY

The approach presented in this paper is based on normalization for fingerprint registration by non-minutiae correlation methods.

3.1. Correlation Methods

The most sustainable to various types and modalities of images are correlation methods. In such methods, the concept of similarity of images is introduced (this is how the correlation methods differ from each other). And further for the registered fingerprint image, the best transformation option is selected in such way that the transformed and target fingerprint images are the most similar. In this paper, we use mutual information (Maes, Vandermeulen & Suetens, 2003) as a similarity metrics. Method Maximizing Mutual Information (MMI) is one of the most common entropy correlation methods. Entropy methods do not depend on the nature of the image, since they work mainly with image histograms.

MMI use some optimized version of the search for the maximum value of the (Zhao et al., 2014). One of the most obvious and effective ways to optimize is to look for an approximate maximum on the grid, and then refine the meaning with a full search or reduce the image several times and apply the algorithm to them, and after registering the reduced copies, refine the result on the original images.

Similar optimizations can be made, since the mutual information increases smoothly when it approaches the desired point (Maes, Vandermeulen & Suetens, 2003). An example of the change in MI, when the image is shifted along the x and y axes, is shown in Fig. 2.
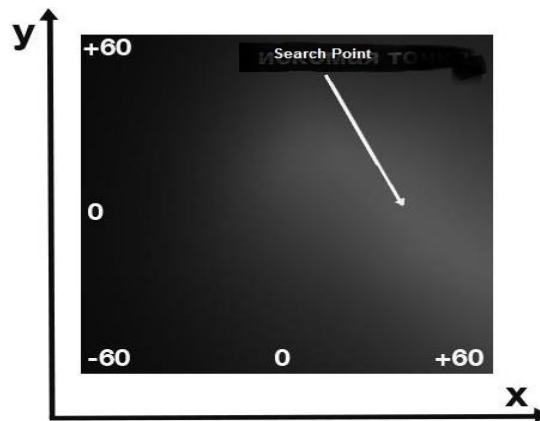

Fig. 2. Graph dependent on mutual information on the displacement of the fingerprint along the x and y axes

Thus, it is possible to make such optimization if the following question is answered. How many times the image can be reduced without losing the accuracy of registration? This paper answers the questions of such estimates by using the method of empirical modes.

3.2. The Method of Empirical Modes

Empirical Mode Decomposition (EMD) was developed in 1998 and its application can be find in many studies (Bhuiyan, Adhami & Khan, 2008; Guryanov & Krylov, 2017). It allows you to analyze nonlinear and non-stationary data and obtain a frequency distribution of data over time for one-dimensional signals by decomposing the signal into functions of different frequencies. An empirical mode is a function with the following properties:

1. For the considered interval, the number of extrema does not differ by more than one, from the number of intersections of zero.
2. The Half-Sum of the upper and lower envelopes of a given function is close to zero.

As a result of signal *f(t)* into empirical modes, we get the following sum:

$$f(t) = r(t) \sum_i^N \phi_i(t), \tag{1}$$

where $\varphi_i(t)$ are empirical modes, and $r(t)$ is the remainder. The first modes contain high frequency characteristics of the signal, and the latter and the remainder are low-frequency characteristics.

3.2.1. Fast decomposition algorithm

There are different methods of decomposing the signal into empirical modes. In this paper, we use the fast adaptive decomposition method for empirical modes (Bhuiyan, Adhami & Khan, 2008). The decomposition algorithm for the one-dimensional signal *I*, consists of the following steps:
1. We set the initial window size to $w = 3$.
2. We find the signal *I* local extremes by search window of size equal to *w*. The local Maxima *p* must satisfy the following conditions:

$$I(p) > I(q), \forall q \in W_w(p), \tag{2}$$

where $W_w(p)$ denotes the window centered at *p* and *w*. Then the local Minima *q* must satisfy the following conditions:

$$I(p) < I(q), \forall q \in W_w(p). \tag{3}$$

3. For each local Maxima, we find the distance to the next nearest maximum and denote this distance by d_{max}. Then for each local Minima, we find the distance to nearest mnimum and denote it by d_{min}. Find the minimum of these values $d = \min(d_{max}, d_{min})$.
4. Update the window size $w = 2 + [^d/_2] + 1$.
5. Compute the upper U and the lower L envelope with updated window size *w*:

$$U(p) = \max_{q \in W_w(p)} I(q), L(p) = \min_{q \in W_w(p)} I(q), \tag{4}$$

6. We calculate the average envelope arithmetic mean R for the upper and lower envelopes with blur window size w:

$$R(p) = \frac{1}{w} \sum_{q \in W_w(p)} \frac{U(q) + L(q)}{2}. \tag{5}$$

23

7. For signal *I*, calculate the empirical mode *M = I - R*. We get high-frequency empirical mode *M* and the low-frequency residual *R*.
8. Next, we assume *I = R* and repeat steps 2–7 (each time we get the next internal mode) until R becomes impossible (i.e. when R has less than two maxima or minima).

3.2.2. Window Size

In the decomposition algorithm described above, the size of the window *w* plays an important role. The window size at each step is the distance between extremes of the same type (Minima or Maxima). The higher the number of empirical mode, low is the frequency. This means that for each next internal mode, the number of extrema will decrease, and the distance between them will increase. The window size for each empirical mode will also increase. Moreover, *w* is an important characteristic of the signal, since by reducing the signal frequency by a factor of *w*, we do not lose local extrema.

4. THE METHOD OF MAXIMIZATION OF MUTUAL INFORMATION

The method of maximizing mutual information is a correlation method of recording images, which is described by the following formula:

$$t^* = \arg\max_t \sum_{u,v} H_{I,J}(u,v) \log \frac{H_{I,J}(u,v)}{H_I(u)H_J(v)}, \qquad (6)$$

Where H_I and H_J are the normalized histograms of the signals *I* and *J*, respectively:

$$H_I(u) = \frac{\left|\{p \in domI : I(p) = u\}\right|}{N_I}, \qquad (7)$$

$$H_J(u) = \frac{\left|\{p \in domJ : J(p) = v\}\right|}{N_J}, \qquad (8)$$

And H_{ItJ} the normalized joint histogram of the signals I_t and *J*:

$$H_{I,J}(u,v) = \frac{\left|\{p \in domJ : I_t(p) = u, J(p) = v\}\right|}{N_J}, \qquad (9)$$

This method is widely used for combining images.

5. OPTIMIZATION OF MMI METHOD

We will consider the example using the above described approach of signal decomposition by the method of empirical modes. It is possible to optimize the correlation methods for registering the fingerprint images.

5.1. Reduction to a one-dimensional signal and its decomposition

It can be seen from the examples of fingerprints (Figure 3) that the important characteristics of the fingerprints under consideration are its orientation field.
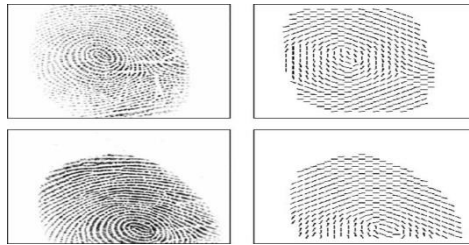

Fig. 3. Shows the orientation filed of two same fingerprint images.

Select orientation field of fingerprints and based on the characteristics of the orientation field, we will draw a conclusion about how many times we can reduce the size of fingerprints without losing the accuracy of registration. First, we construct a binary mask of the fingerprint from the image of the fingerprint. The mask is constructed using a luminance thresholding with complementary morphological analysis to remove the gaps inside the mask and the extra elements outside the fingerprint. The data were taken from (Sharat, 2005). An example of a mask and its fingerprint for this fingerprint is shown in Figure. 4.

(a)   (b)

Fig. 4. Mask of Fingerprint(a) and Fingerprint (b)

Further, we translate these masks into a polar coordinate system with a reference to core of the fingerprint and move from 2D picture to one-dimensional signal. The result of such a transition is shown in Figure 4. Now we decompose the resulting one-dimensional signal using the fast adaptive method of empirical modes.
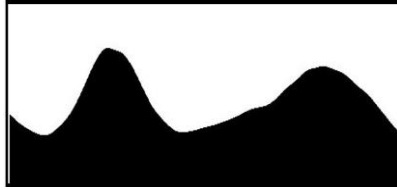
Fig. 5. The inverted Mask

The result of decomposition of fingerprints in Figure 6, can be seen in Figure 7. We are interested in the size of the window w, obtained after each Empirical Mode.

(a)   (b)   (c)

Fig. 6. Fingerprints from Database FVC2002
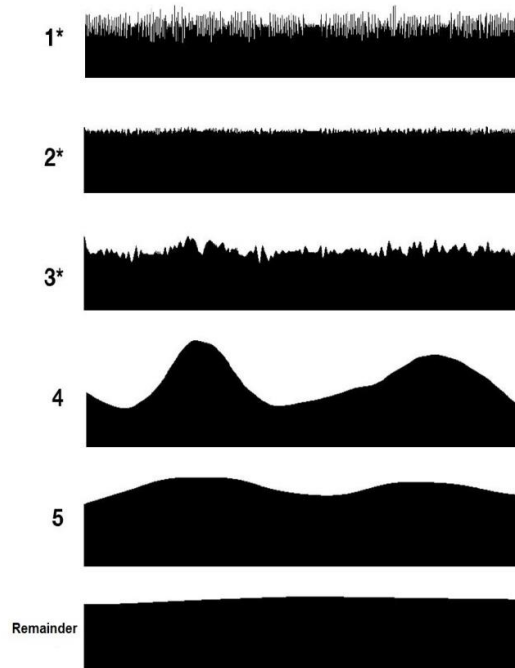

1*

2*

3*

4

5

Remainder

Fig. 7. The result of decomposition by the method of Empirical Signal Modes (modes marked with an asterisk (*) are scaled for clarity)

5.2. Computing the Reduction Ratio of a Fingerprint

Table 1 reflects the important properties of the algorithm (Guryanov & Krylov, 2017). The Jump in Window size is determined by the following formula:

$$k \rightarrow \min : \frac{\ln(w_{k+1})}{\ln(w_k)} \geq \frac{\ln(w_{i+1})}{\ln(w_i)}, \forall i. \tag{10}$$

Tab. 1. Dependence of the window size on the internal mode number for the three test images

Modes / Images	1	2	3	4	5	6	7
a	3	3	**10**	220	262	5	3
b	3	3	7	**9**	51	180	300
c	3	3	3	**10**	72	240	312

Further, internal modes after the jump in the window size contain the lowest-frequency characteristics of the fingerprint. For the purpose of reducing the size of registered images, we will choose an Empirical Mode directly before the jump in the size of window. This Empirical Mode contains the most important high-frequency characteristics, since noise and other random extremes are eliminated in the calculation from the first Empirical Mode. Therefore, the main parameter for calculating the image reduction factor, we take the window size w corresponding to this Empirical Mode. Now using the window size w, we calculate the image reduction factor k as follows:

$$k = \frac{\pi w (width + height)}{4N}. \tag{11}$$

Where width and height are respectively the width and height of the fingerprint, and N is the number of steps by angle parameter, while passing to a one-dimensional signal from the polar coordinate system. We translate w from the polar coordinate system, back to the Cartesian coordinate system and into pixels. Therefore, the value depends on the image dimensions and on the number of steps by angle parameter. The obtained parameter k is used to optimize the selection of transformation to Maximize Mutual Information.

6. RESULTS OF OPTIMIZATION STAGE

We tested the proposed method on a set of images. To estimate the acceleration coefficient of the Algorithm instead of a full search for transforming the angle and shifts along the x and y, we looked first for a maximum of mutual information on the grid with step k. The computation time is reduced to k^3 times. The results of the algorithm for different pairs of images are shown in Table 2.

Tab. 2. The fingerprints marked with (*) were computed on the proposed algorithm of Normalization

	X	Y	Angle	Scale	Coef.	Time (s)
Fingerprint 1	40	-10	-25	1.15	–	5100
Fingerprint 1*	40	-10	-25	1.15	8	20
Fingerprint 2	4	18	-8	1	–	4900
Fingerprint 2*	4	18	-8	1	8	26
Fingerprint 3	-40	-11	25	0.85	–	4780
Fingerprint 3*	-40	-11	25	0.85	9	21

It can be seen that while applying the optimization, the images registration result do not change. This significantly reduces the running time of the algorithm. It can be seen that our estimate of the acceleration coefficient was adequate. Thus, it can be argued that the resulting estimation of the optimization factor is successful, since we significantly speed up the registration process and do not degrade the quality of the method of Maximizing Mutual Information.

Further the normalized fingerprints were tested on matching Algorithms. Three correlation matching algorithms were considered. Table 3 contains the details of these algorithms.

Tab. 3. The Matching Algorithms

Author	Technique	Feature
Jain, Hong & Bolle, 1997	Correlate **(Correlation Matching)**	Finger codes
Sharat, 2005	Chain code **(Correlation Matching)**	Binary image
Bansal, Sehgal, & Bedi, 2011	Flow ridge **(Correlation Matching)**	Ridge uses flow

The performance of these algorithms on quality fingerprint images was very good but when tested on fingerprints of poor quality in databases FVC2002, FVC2004 and FVC2006, their Equal Error Rate (EER) were more than 50%. EER is the spot where False Match Rate (FMR) becomes equal to False Non-Match Rate (FMNR).

The same poor quality images when optimized by our algorithm and again tested on these algorithms, their performance improves a lot. Table 4 shows the result of these experiments.

Tab. 4. The Results of poor quality/Latent images when the proposed algorithm is applied

Algorithm	Results %	Average Run Time (ms)
Correlate **(Correlation Matching)**	EER = 45%	586
Chain code **(Correlation Matching)**	EER = 42%	168
Flow ridge **(Correlation Matching)**	EER = 46%	135

7. CONCLUSION

The algorithm proposed in this paper for optimization of fingerprint size is very powerful, and solve many problems of conventional fingerprint verification techniques. Specially the techniques performs strongly for latent fingerprint. By using orientation information for registration, the alignment is not strictly based on trying to maximize the number of minutiae correspondences.

The algorithm for estimating the possible reduced size of registered images, accelerate the correlation methods of image registration. The algorithm was tested to optimize the method of maximizing mutual information.

The experiments showed good results on a set of poor quality fingerprints. We were able to substantially improve the speed of the comparison algorithms without degrading the quality of registration.

REFERENCES

Bansal, R., Sehgal, P., & Bedi, P. (2011). Minutiae Extraction from Fingerprint Images – a Review. *IJCSI International Journal of Computer Science Issues*, *8*(5), 74–85.

Bazen, A., Verwaaijen, G., Gerez, S., Veelenturf, L., & Zwaag, B. (2000). A correlation-based fingerprint verification system. In: *Proceedings of the Workshop on Circuits Systems and Signal Processing* (pp. 205–213). Veldhoven, The Netherlands.

Bhuiyan, S. M. A., Adhami, R. R., & Khan, J. F. (2008). A novel approach of fast and adaptive bidimensional empirical mode decomposition. In *IEEE International Conference on Acoustics, Speech and Signal Processing* (pp.1313–1316). Las Vegas, NV. doi:10.1109/ CASSP.2008.4517859

Guryanov, F., & Krylov, A. S. (2017). Fast medical image registration using bidirectional empirical mode decomposition. *Signal Processing: Image Communication*, *59*, 12–17. doi:10.1016/ .image.2017.04.003

Yager, N., & Amin, A. (2004). Fingerprint verification based on minutiae features: a review. *Pattern Analysis and Applications*, *7*(1), 94–113. doi:10.1007/s10044-003-0201-2

Jain, A., Hong, L., & Bolle, R. (1997). On-line fingerprint verification. *IEEE Transactions on Pattern Analysis and Machine Intelligence*, *19* (4), 302–314. doi:10.1109/34.587996

Jiang, X., & Yau, W. (2000). Fingerprint minutiae matching based on the local and global structures. In: *Proceedings 15th International Conference on Pattern Recognition. ICPR-2000* (pp. 1038–1041). Barcelona, Spain. doi: 10.1109/ICPR.2000.906252

Maes, F., Vandermeulen, D., & Suetens, P. (2003). Medical Image Registration Using Mutual Information. *Proceedings of the IEEE*, *91*(10), 1699–1722. doi:10.1109/JPROC.2003.817864

Park, C., Lee, J., Smith, M., Park, S., & Park, K. (2004). Directional filter bank-based fingerprint feature extraction and matching. *IEEE Transactions on Circuits and Systems for Video Technology, 14*(1), 74–85. doi:10.1109/TCSVT.2003.818355

Ratha, N., Karu, K., Chen, S., & Jain, A. (1996). A real-time matching system for large fingerprint databases. *IEEE Transactions on Pattern Analysis and Machine Intelligence*, *18*(8), 799–813. doi:10.1109/34.531800

Sharat, S. C. (2005). *Online fingerprint Verification System* (Unpublished dissertation). University of New York Buffalo, USA.

Zhao, Y., Yao, R., Ouyang, L., Ding, H., Zhang, T., Zhang, K., Cheng, S., & Sun, W. (2014). Three-Dimensional Printing of Hela Cells for Cervical Tumor Model in Vitro. *Biofabrication*, *6*(3), 035001. doi:10.1088/1758-5082/6/3/035001

Quirino ESTRADA [0000-0003-0623-3780]*, *Dariusz SZWEDOWICZ**,
*Julio C. VERGARA**, *José SOLIS***, *Miguel A. PAREDES***,
Lara WIEBE, *Jesús M. SILVA**

NUMERICAL SIMULATIONS OF SANDWICH STRUCTURES UNDER LATERAL COMPRESSION

Abstract

The current paper analyzes the effect of the cross-section on the energy absorption capabilities of sandwich structures under compressive loads. For this purpose, several cross-section including triangular, square, hexagonal and circular shapes were analyzed using Abaqus software. According to the results the hexagonal shape is the most favorable cross-section to increase the crashworthiness performance of the structures up to 700% of CFE with respect to the square arrangement.

1. INTRODUCTION

From the high safety standards for passengers, the crashworthiness performance is the most important requirement in automotive, aerospace and rail industry (Zhang, Xu, Wang, Chen & Wang, 2018). Thus, the structural designs should provide a controlled deceleration of the vehicles in order to reduce the injuries of the occupants during crash events. The use of thin-walled structures is widely used to tackle this harmful effect. The absorption of the energy is raised when the

---

* Universidad Autónoma de Ciudad Juárez, Instituto de Ingeniería y Tecnología, Av. Plutarco Elías Calles, Fovissste Chamizal, 32310, Ciudad Juárez, Chihuahua, México, quirino.estrada@uacj.mx, lara.wiebe@uacj.mx, jesilva@uacj.mx
** Centro Nacional de Investigación y Desarrollo Tecnológico/TecNM, Departamento de Ingeniería Mecánica, Interior Internado Palmira, 62490, Cuernavaca, Morelos, México, d.sz@cenidet.edu.mx, julio.vergara17ma@cenidet.edu.mx
*** Instituto Tecnológico de Tlalnepantla, División de Estudios de Posgrado e Investigación, Av. Instituto Tecnológico, la Comunidad, 54070 Tlalnepantla de Baz, Estado de México, jsolis@ittla.edu.mx

structures are plastically deformed. The crashworthiness performance is a function of many parameters such as geometry, cross-section, material and arrangement of the structures. In this way, several thin-walled structures have been studied such as single (Goel, 2015), bi-tubular (Estrada et al., 2019), multicell and sandwich/ honeycomb arrangements (Ivañez, Fernandez-Cañadas & Sanchez-Saez, 2017). In all cases, such structures are an effective and low-cost alternative to absorb energy during crash events. Moreover, honeycomb arrangements allow an increase of crashworthiness capabilities in relation to other kinds of structures (Crupi, Epasto & Guglielmino, 2013). A typical sandwich structure is formed by a core between two face sheets (Li & Wang, 2017). Considering the orientation of the panel with respect to the load direction, the honeycomb structures can be crushed in-plane and out-of-plane direction. In both cases, different crash-worthiness performances are obtained. In this context (Khan, Baig, & Mirza, 2012) it is reported an experimental investigation that deals with in-plane and out-of-plane crushing of aluminum alloy 3003 honeycomb structures. The local and global plastic strains were obtained by digital image correlation. It was concluded that the out-of-plane direction presented the highest energy absorption. Considering in-plane crashworthiness behavior, many studies have focused their efforts to analyze different core topologies. However, triangular configuration exhibits a better crashworthiness performance of bio-inspired hierarchical honeycombs, (Yin, Huang, Scarpa, Wen, Chen & Zhang, 2018). Furthermore, for in out-of-plane direction, it was analyzed the energy absorption capabilities of bio-inspired aluminum honeycomb with horseshoe mesostructured, (Yang, Sun, Yang, & Pan, 2018). The horseshoe shapes were built based on triangle, square, hexagon and kagome honeycomb structures. To compare with typical honeycomb structures the horse-shaped honeycomb obtained the best energy absorption performance. Considering filled materials, the authors of (Liu et al., 2017) evaluated the crushing response of aluminum honeycombs panels filled with expanded polypropylene (EPP) foams. The compression tests were conducted in axial (out of plane) and lateral (in plane) direction. For the axial configuration the EPP foam increased the crashworthiness performance of the structures compared to the empty honeycomb panels in a range of 43 to 120%. Moreover, a better improvement was found for energy absorption in lateral crushing up to 30397%. Finally, the study of crushing of honeycomb structures in-plane and out-of-plane has been extensively reported. However, the study of honeycomb structures under in-plane crushing direction is barely reported.

Thus, the current article studies the effect of the cross-section on the crash-worthiness performance of sandwich structures in-plane crushing direction. For this purpose, several numerical simulations were carried out using Abaqus finite element software. The evaluated cellular cores are based on triangular, square, hexagonal and circular shapes. In all cases, the structures were made with aluminum AA 6063-T5 and using same mass value.

2. MECHANICAL CHARACTERIZATION OF ALUMINUM ALLOY 6063-T5

The use of light materials is one of the most important requirements in the crashworthiness design of vehicles. In order to guarantee an optimal strength/weight ratio of the structural components, the use of aluminum alloys is widely used. AA 6063-T5 exhibited an excellent mechanical behavior and great resistance to corrosion (Zhu, Qin, Wang & Qi, 2011). Thus, all evaluated structures in this study are made with AA6063-T5. The mechanical characterization was carried out following the tensile test ASTM7-E8 for rectangular specimens. An AG-X plus 100kN Shimadzu universal test machine with a quasi-static velocity of 2 mm/min was used for the tensile tests. Details of the tensile specimens are depicted in Figure 1.
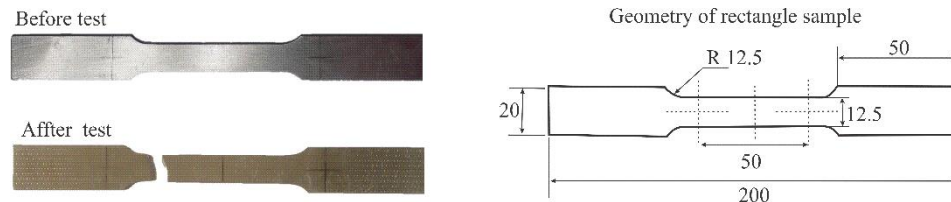

Fig. 1. Tensile sample for ASTM7-E8 (units in mm)

The mechanical response of the specimen is shown in Figure 2. From this curve, the mechanical characterization of AA6063-T5 was carried out. The parameters used in Abaqus models are listed in Table 1, which are consistent with previous works, (Wang, Li & Zhang, 2016). Due to quasi-static nature of the tensile test besides of small strain rate sensitivity of 6063-T5 alloy in a range of 10^{-4} to 10^{3} s^{-1}, the strain rate effects were neglected, (Smerd, Winkler, Salisbury, Worswick, Lloyd & Finn, 2005).
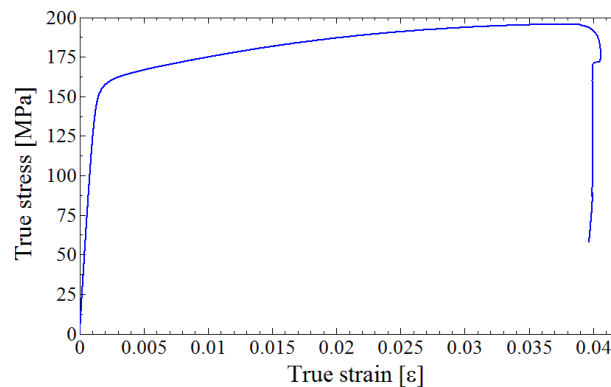

Fig. 2. Force-displacement curve for AA6063-T5

33

Tab. 1. Mechanical properties for AA6063-T5

	Young modulus [MPa]	Poisson coefficient	Density [kg/m^3]
Elasticity	66940	0.33	2700
Plasticity	Yield stress S_y [MPa]		
	158.79		

3. FIRST NUMERICAL MODEL WITH EXPERIMENTAL VALIDATION

Given that our study is of numerical kind, a first model designated as (S-00) worked out using Abaqus/explicit was conducted. The numerical model was validated through a quasi-static compression test utilizing a universal test machine at 6 mm/min. The discrete model was developed with the assumption that the core of the sandwich panel is obtained from the joint of several single profiles. In this way, the discrete model describes a single square profile subjected to in-plane compression (lateral). The profile was built with AA6063-T5 and height (H) of 38.3 mm, length (L) of 130 mm and thickness (t) of 1.4 mm. The tube was modeled using S4R shell elements with elastoplastic properties described in Table 1. Meanwhile R3D4 elements were used to model the compressed plates as rigid bodies. During the compression test, the structure was set between two rigid plates in lateral direction. A contact interaction with friction coefficient of μ = 0.3 was implemented, (Zhang, Zhang & Wang, 2016). From experimental validation and mesh convergence analysis, an element of 2.5 mm was implemented. Therefore, a total number of 3120 elements were generated. Details of the physical and numerical models are described in Figure 3.
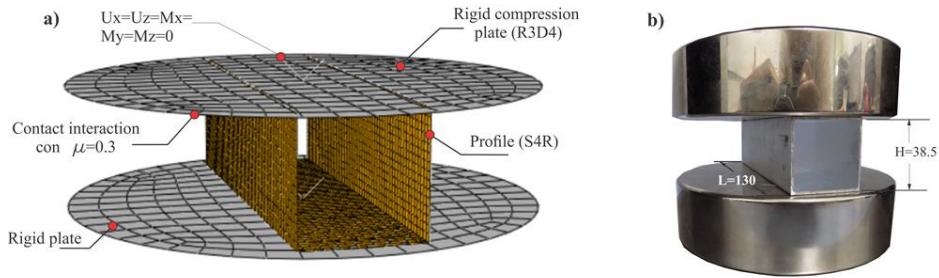

Fig. 3. Lateral compression of S-00 profile: a) discrete model and b) experimental model

The force-displacement curves for both cases were obtained and are compared as shown in Figure 4. In the same plot, the results for the mesh convergence analysis also are presented. In this sense, coarse (5 mm), medium (2.5 mm) and fine (1 mm) meshes were evaluated. Despite of the numerical curves present very little difference, when a zoom on P_{max} region is made a convergence criterion

34

is obtained. A difference close to 2% for fine and medium mesh is obtained. This was not the case for the coarse mesh. Thus, the medium (2.5 mm) element size was validated and the corresponding results are discussed below. As it is observed in Figure 4, the discrete model correctly represents the compression behavior of the structure in quantitative and qualitative way. In this sense, the numerical results predicted a P_{max} value of 46.67 kN and energy absorption of 0.133 kJ, which represents a difference of 1.01% and 3 %, with respect to experimental setup. This discrepancy is associated to the complexity when the plastic deformation involving contact phenomena is captured. In Figure 5 as the compression is carried out the contact area changes from plane to line condition. With regard to the mechanical behavior (see Fig. 4) this is characterized by an increase of compression force until a maximum value of P_{max}~47 kN. Subsequently, the failure of the structure is reached, provoking a drastic drop of the force within the first 2 mm. Afterwards, a smooth decrease is obtained along the compression procedure (20 mm), which is stopped to reach a compression force equal to 5 kN.
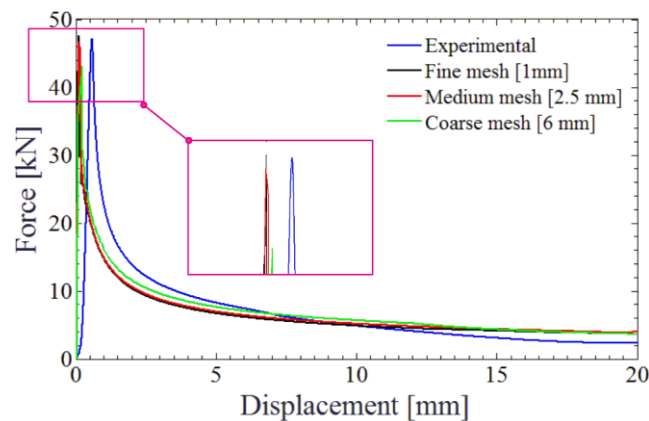

Fig. 4. Comparison of force displacement-curves for first discrete model (S-00)

The final deformation state is presented in Figure 5. The discrete model captured correctly the experimental collapsing mode of the structure. Considering the cross-section, the plastic deformation initiated with the formation of a hinge-line along the length of the profile at middle height. After that, a rolling inside effect on vertical edges was noticed. As the rolling effect increased, the top edge suffers a concave plastic deformation. Opposite deformation occurred at the bottom edge.
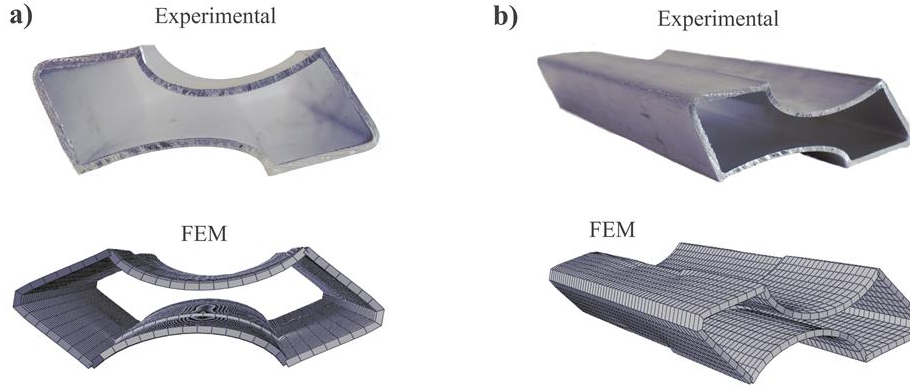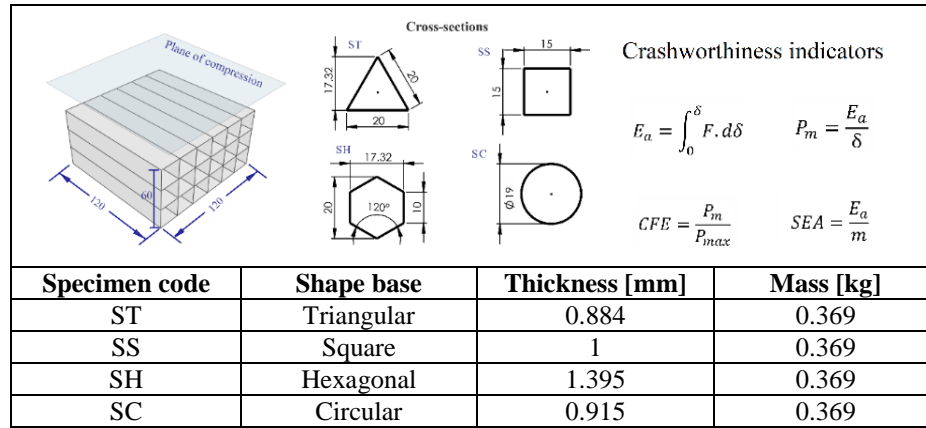
Fig. 5. Final deformation state: a) is the cross-section and b) the isometric view

Lastly, according to Figure 4 and 5 the numerical model describes the mechanical behavior of the profile in the quantitative and qualitative way. Hence, the discrete model is validated, and we can continue with the study of the effect of the cross-section on crashworthiness performance of sandwich structures under lateral load.

4. NUMERICAL SIMULATIONS

The main contribution of this paper was to analyze the effect of the cross-section of sandwich structures when are subjected to quasi-static lateral compression. For this purpose, numerous simulations were carried out. The analyzed cross-sections included triangular, square, hexagonal and circular shapes. In order to get a reliable comparison, all sandwich arrangements presented same mass (0.369 kg) and were made with an aluminum 6063-T5 alloy. The assessment of the structures was carried out by dimensional and dimensionless crashworthiness parameters. The most important are as follows: the peak load (P_{max}), the energy absorption (E_a), the mean crush force (P_m), the crush force efficiency (CFE) and the specific energy absorption (SEA). Where F is the compression force, δ the displacement and m the mass. The E_a was obtained by integration of the area under force vs displacement curves, using an integration method known as trapezium rule. Regarding the CFE, optimal performance of the structure is obtained when CFE equals to 1. Details of the evaluated specimens and crashworthiness parameters are shown in Table 2.
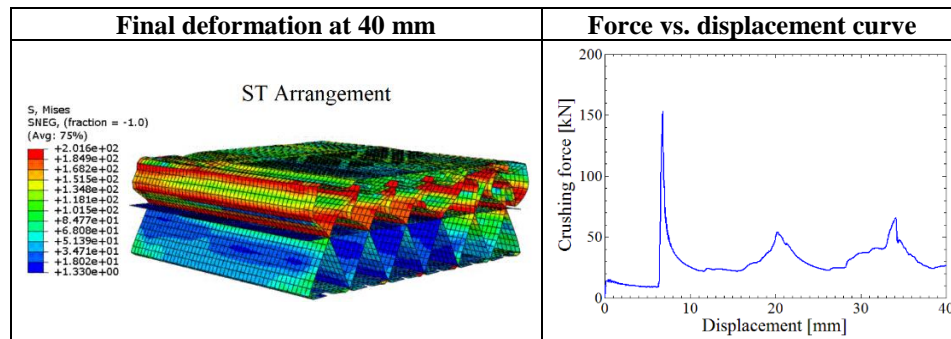
Tab. 2. Numerical setup (dimensions in mm)

Cross-sections

Crashworthiness indicators

$$E_a = \int_0^\delta F.d\delta \qquad P_m = \frac{E_a}{\delta}$$

$$CFE = \frac{P_m}{P_{max}} \qquad SEA = \frac{E_a}{m}$$

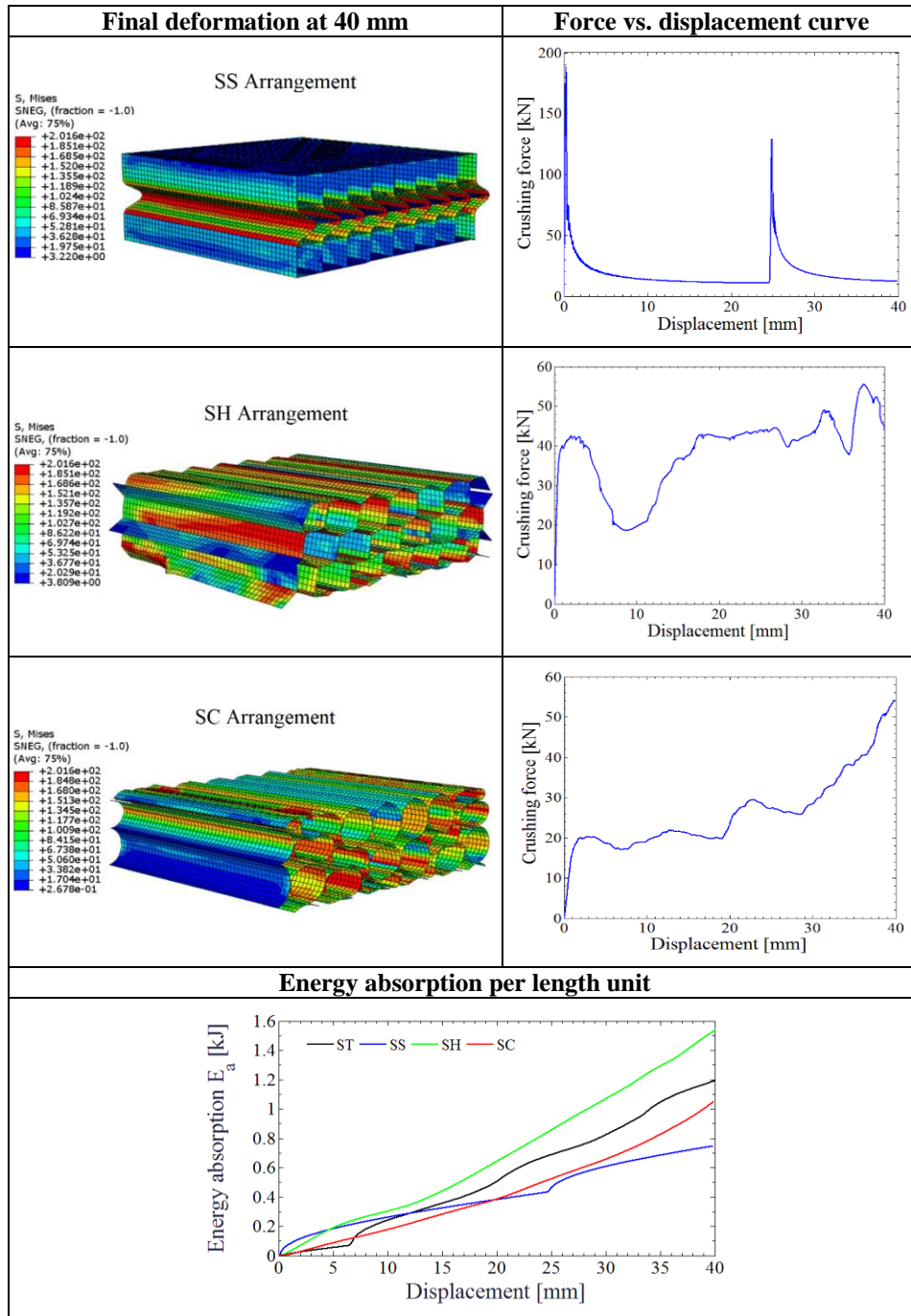| Specimen code	Shape base	Thickness [mm]	Mass [kg]
ST	Triangular	0.884	0.369
SS	Square	1	0.369
SH	Hexagonal	1.395	0.369
SC	Circular	0.915	0.369

5. RESULTS

The crashworthiness performance of the structures was obtained from the analysis of the crushing force vs. displacement curves. The structures with triangular and square base exhibited a peak load (P_{max}) value followed by a drop of the crushing force. Meanwhile, the structures close to circular shape described a smooth transition between P_{max} and mean crushing force (P_m). Depending on the cross-section, different values of P_{max} in a range of 188 to 53 kN were calculated. The interaction between the walls of the structures modified the typical deformation mode described for the single profiles (Fan, Hong, Sun, Xu & Jin, 2015). Hexagonal and circular profiles presented higher deformation than triangular and square sandwich structures, as can be seen in Table 3 and 4. This was corroborated observing the plot of the energy absorption (E_a) along with the displacement (see Table 4). Hexagonal and circular cross-section, in turn, presented higher stability during the compression test.

Tab. 3. Mechanical behavior of the sandwich structures I

Final deformation at 40 mm	Force vs. displacement curve

Tab. 4. Mechanical behavior of the sandwich structures II

Final deformation at 40 mm	Force vs. displacement curve
SS Arrangement	
SH Arrangement	
SC Arrangement	
Energy absorption per length unit	

A summary of crashworthiness results of the whole evaluated sandwich arrangements is compiled in Table 5. The energy absorption (E_a) performance of the structures was directly influenced by the cross-section. The best E_a was obtained for hexagonal structures (SH) with 1.553 kJ, which represents an increase of 108.17% respect to the lowest E_a value for the HS profile. (0.746 kJ). This behavior was verified by calculating the maximum mean crush force (P_m) and specific energy absorption (SEA) equal to 38.82 kN and 4.20 J/gr, respectively. On the other hand, the poorest crashworthiness performance was achieved for the triangular sandwich structure (ST). This condition is associated to small deformation besides of the apparition of the buckling phenomena.

Tab. 5. Mechanical behavior of the honeycomb structures

Code	P_{max} [kN]	P_m [kN]	E_a [kJ]	SEA [J/gr]
ST	153.33	29.82	1.193	3.23
SS	188.81	18.65	0.746	2.02
SH	55.44	38.82	1.553	4.20
SC	53.50	25.80	1.049	2.84

A high E_a value does not necessarily represent the best crashworthiness performance. In this way, the crushing force efficiency (CFE) is a more useful parameter. The CFE involves a comparison of the P_m and P_{max} values. An optimal behavior of the profiles is achieved when the CFE value is close to the unit. A comparison of CFE values for all sandwich arrangements is shown in Figure 6.
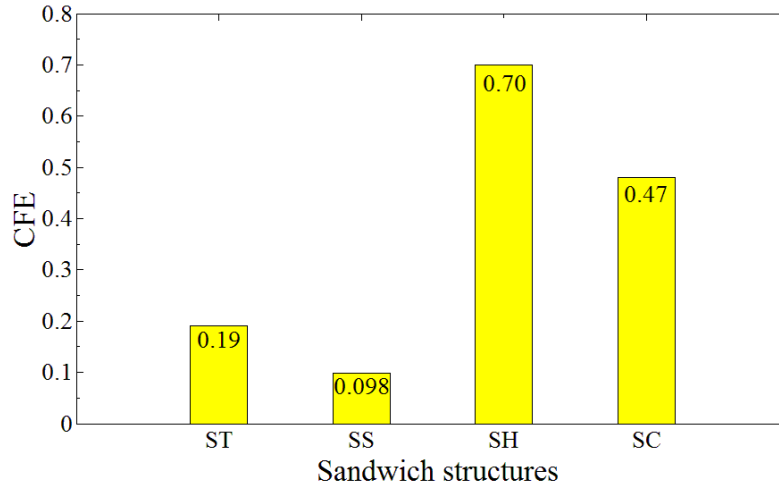

Fig. 6. Comparison of CFE parameter for all evaluated structures

According to Figure 6, cross-sections with many edges or close to the circular shape show a better CFE performance. In this way, two trends were described by the structures. The first is formed by structures ST and SS, which is characterized by low CFE values close to 0.2. This condition was obtained due to a high P_{max} value at the beginning of the crushing process, followed for a drastic drop to the crush force. The opposite case was observed for structures SH and SC where only minor differences between P_{max} and P_m were calculated. Therefore, higher CFE values were achieved. The best CFE value of 0.70 was obtained for the sandwich structure with hexagonal base. This means an increase of 700% respect to the lowest CFE value (0.1). The hexagonal cross-section allowed for high resistance to form the plastic hinge lines with a great stability of the arrangement during all crushing process. Thus, profiles with hexagonal cross-section should be considered to the control of lateral impacts.

6. CONCLUSION

A numerical study of the effect of the cross-section on the crashworthiness performance of sandwich structures under lateral load was carried out. According to our study, the following conclusions were obtained:

1. Considering the same mass for all structures (369 g), the energy absorption (E_a) is highly dependent on the arrangement of the single profiles in the cross-section. In second instance, the E_a depends on the geometrical base of these profiles. This condition explains the higher E_a value for the triangle specimen respect to the square sandwich profile.
2. The E_a capabilities can be improved when hexagonal cross-section is implemented. In this way, an increase of 108% was calculated in relation to the lowest value that was calculated for square sandwich structure (0.746 kJ).
3. As the cross-section tends to form a circular shape, a decrease in the peak load (P_{max}) value was computed. The lowest P_{max} value ~53.50 kN was obtained by the sandwich structure with circular base (SC).
4. Regarding to CFE parameter, a better performance is obtained when the cross-section tends to form hexagonal or circular shape. Then, an improvement in a range from 480% to 700 % can be achieved.
5. Square and triangular cross-section are not recommended to design energy absorption systems due to the high P_{max} values and the instability presented during crushing process.
6. Finally, hexagonal honeycomb structure presents the best crashworthiness performance with a CFE value equal to 0.70. This means an excellent stability with a large plastic deformation. This kind of structure can be used to reduce injuries and fatalities during axial impacts.

REFERENCES

Crupi, V., Epasto, G., & Guglielmino, E. (2013). Comparison of aluminium sandwiches for lightweight ship structures: Honeycomb vs. foam. *Marine Structures*, *30*, 74–96. doi:10.1016/J.MARSTRUC.2012.11.002

Estrada, Q., Szwedowicz, D., Rodriguez-Mendez, A., Elías-Espinosa, M., Silva-Aceves, J., Bedolla-Hernández, J., & Gómez-Vargas, O. A. (2019). Effect of radial clearance and holes as crush initiators on the crashworthiness performance of bi-tubular profiles. *Thin-Walled Structures*, *140*, 43–59. doi:10.1016/J.TWS.2019.02.039

Fan, H., Hong, W., Sun, F., Xu, Y., & Jin, F. (2015). Lateral compression behaviors of thin-walled equilateral triangular tubes. *International Journal of Steel Structures*, *15*(4), 785–795. doi:10.1007/s13296-015-1202-x.

Goel, M. D. (2015). Deformation, energy absorption and crushing behavior of single-, double- and multi-wall foam filled square and circular tubes. *Thin-Walled Structures*, *90*, 1–11. doi:10.1016/J.TWS.2015.01.004

Ivañez, I., Fernandez-Cañadas, L. M., & Sanchez-Saez, S. (2017). Compressive deformation and energy-absorption capability of aluminium honeycomb core. *Composite Structures*, *174*, 123–133. doi:10.1016/J.COMPSTRUCT.2017.04.056

Khan, M. K., Baig, T., & Mirza, S. (2012). Experimental investigation of in-plane and out-of-plane crushing of aluminum honeycomb. *Materials Science and Engineering: A*, *539*, 135–142. doi:10.1016/J.MSEA.2012.01.070

Li, T., & Wang, L. (2017). Bending behavior of sandwich composite structures with tunable 3D-printed core materials. *Composite Structures*, *175*, 46–57. doi:10.1016/J.COMPSTRUCT.2017.05.001

Liu, Q., Fu, J., Wang, J., Ma, J., Chen, H., Li, Q., & Hui, D. (2017). Axial and lateral crushing responses of aluminum honeycombs filled with EPP foam. *Composites Part B: Engineering*, *130*, 236–247. doi:10.1016/J.COMPOSITESB.2017.07.041

Smerd, R., Winkler, S., Salisbury, C., Worswick, M., Lloyd, D., & Finn, M. (2005). High strain rate tensile testing of automotive aluminum alloy sheet. *International Journal of Impact Engineering*, *32*(1–4), 541–560. doi:10.1016/J.IJIMPENG.2005.04.013

Yang, X., Sun, Y., Yang, J., & Pan, Q. (2018). Out-of-plane crashworthiness analysis of bio-inspired aluminum honeycomb patterned with horseshoe mesostructure. *Thin-Walled Structures*, *125*, 1–11. doi:10.1016/J.TWS.2018.01.014

Yin, H., Huang, X., Scarpa, F., Wen, G., Chen, Y., & Zhang, C. (2018). In-plane crashworthiness of bio-inspired hierarchical honeycombs. *Composite Structures*, *192*, 516–527. doi:10.1016/J.COMPSTRUCT.2018.03.050

Wang, Z., Li, Z., & Zhang, X. (2016). Bending resistance of thin-walled multi-cell square tubes. *Thin-Walled Structures*, *107*, 287–299. doi:10.1016/J.TWS.2016.06.017

Zhang, Y., Xu, X., Wang, J., Chen, T., & Wang, C. H. (2018). Crushing analysis for novel bio-inspired hierarchical circular structures subjected to axial load. *International Journal of Mechanical Sciences*, *140*, 407–431. doi:10.1016/J.IJMECSCI.2018.03.015

Zhang, X., Zhang, H., & Wang, Z. (2016). Bending collapse of square tubes with variable thickness. *International Journal of Mechanical Sciences*, *106*, 107–116. doi:10.1016/J.IJMECSCI.2015.12.006

Zhu, H., Qin, C., Wang, J. Q., & Qi, F. J. (2011). Characterization and Simulation of Mechanical Behavior of 6063 Aluminum Alloy Thin-Walled Tubes. *Advanced Materials Research*, *197–198*, 1500–1508. doi:10.4028/www.scientific.net/AMR.197-198.1500

Md. Torikur RAHMAN [0000-0003-2173-6458]*

A NOVEL APPROACH TO ENHANCE THE PERFORMANCE OF MOBILE AD HOC NETWORK (MANET) THROUGH A NEW BANDWIDTH OPTIMIZATION TECHNIQUE

Abstract

Now is the age of information technology. World is advancing day by day. At present in this progressing world communication from one place to another has become so easy, less costly, and faster. This modern life is almost impossible with the help of these communication technologies. People need to talk, need to share data, need to express their emotion from long distance. So they need to use technologies to communicate with one another. Nowadays the fields of MANET have yielded more and more popularity and thus MANET have become a subject of great interest for the researchers to enforce research activities. Mobile Ad Hoc Network (MANET) is the cooperative engagement of a collection of mobile nodes without the required intervention of any centralized access point or existing infrastructure. There is an increasing trend to adopt mobile ad hoc networking for commercial uses. Mobile Ad Hoc Network (MANET) is an emerging area of research to provide various communication services to the end users. But these communication services of Mobile Ad Hoc Network (MANET) use high capacity of bandwidth and a big amount of internet speed. Bandwidth optimization is indispensable in various communications for successful acceptance and deployment of such a technology. Thinking of this, I propose a New Bandwidth Optimization Technique that Enhance the Performance of Mobile Ad Hoc Network (MANET). The new Bandwidth optimization technique which is more efficient in terms of time delay in Mobile Ad Hoc Network (MANET) can redirect a new way towards optimization development in network communication and device junction technology.

* Uttara University, Department of Computer Science & Engineering, House–4 & 6, Road–15, Sector–6, Uttara Model Town,Uttara, Dhaka-1230, Bangladesh, torikurrahman@gmail.com

1. INTRODUCTION

A mobile ad hoc network (MANET) sometimes called a wireless ad hoc network or a mobile mesh network is a wireless network, comprised of mobile computing devices (nodes) that use wireless transmission for communication, without the aid of any established infrastructure or centralized administration such as a base station or an access point (Siva Ram Murthy & Manoj, 2004; Basagni, Conti, Giordano & Stojmenovic, 2003). Unlike traditional mobile wireless networks, mobile ad hoc networks do not rely on any central coordinator but communicate in a self-organized way. Mobile nodes that are within each other's radio range communicate directly via wireless links, while those far apart rely on other nodes to relay messages as routers. In ad hoc network each node acts both as a host (which is capable of sending and receiving) and a router which forwards the data intended for some other node. Ad hoc wireless networks can be deployed quickly anywhere and anytime as they eliminate the complexity of infrastructure setup. Applications of ad hoc network range from military operations and emergency disaster relief, to commercial uses such as community networking and interaction between attendees at a meeting or students during a lecture (Aggelou, 2004; Agrawal & Chauhan, 2015). MANET disseminate important and real-time information to the nodes such as weather information, transit systems, internet access, mobile e-commerce, and other multimedia applications. Most of these applications or systems demand high capacity of bandwidth and a big amount of internet speed so that user can communicate among themselves. Most of the previous research on ad hoc networking has been done using exist many technique of bandwidth optimization in mobile ad hoc network (MANET) focusing only upon the efficiency of the network. There are quite a number of bandwidth optimization technique that are excellent in terms of efficiency like Leaky bucket, Token bucket, Traffic smoothing, Traffic burst shaping etc. However more time delay and big amount of packet drop is happen in many scheme like Leaky bucket and Token bucket. In Token bucket method packet drop is happened less than the Leaky bucket but the time delay is relatively more than Leaky bucket algorithm. So in order to improve the performance of mobile ad hoc network (MANET) bandwidth optimization is highly desirable.

In this paper I have put my concern on the working principle, major components and existing bandwidth optimization technique of MANET besides the basic terminologies. Finally, I proposed a new bandwidth optimization technique that Enhance the Performance of Mobile Ad Hoc Network (MANET) which will more stable in terms of time delay in MANET. With the help of the algorithm, it ensures no matter what the packet size is, the delay is relatively less than the existing schemes for a particular data interval time, provides an optimized process. The defined algorithm controlled the bandwidth by transferring data packets through measuring delay time.

2. MOBILE AD HOC NETWORKS

A mobile ad hoc network (MANET) is a wireless network, comprised of mobile computing devices (nodes) that use wireless transmission for communication, without the help of any established infrastructure or centralized administration such as a base station in cellular network or an access point in wireless local area network (Agrawal & Chauhan, 2015). The nodes are free to move randomly and organize themselves arbitrarily; thus, the network's wireless topology may change rapidly and unpredictably. In mobile ad hoc network, each node acts both as a host (which is capable of sending and receiving) and a router which forwards the data intended for some other node (Perkins, 2008). As shown in Figure 1, an ad hoc network might consist of several home-computing devices, including laptops, cellular phones, and so on.
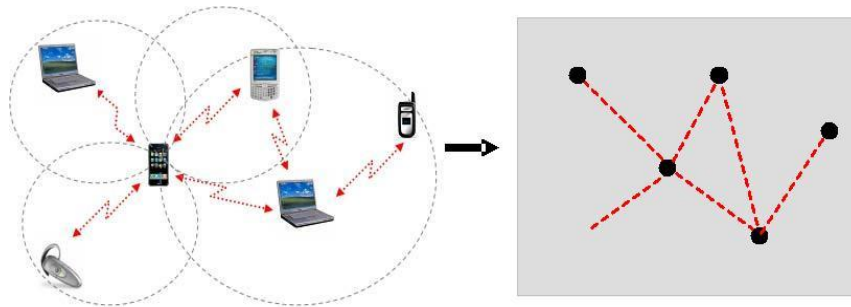

Fig. 1. A Typical Mobile Ad Hoc Network

3. ANALYSIS FOR BANDWIDTH OPTIMIZATION

Bandwidth management is the procedure of managing and controlling the communications (traffic, packets) through measurement on a network link, to ensure the avoidance of flooding the link to its maximum range of capacity or over flooding the link, which would result in a network congestion and poor performance within the network. It is measured in bits per second (bit/s) or bytes per second (B/s) (Pujolle, 2013).

Bandwidth optimization is a procedure that can measure and utilize the capacitive bandwidth within the whole system. Now a day's bandwidth management is a problem as the number of internet users are increased day by day. Even using local LAN, a limit of bandwidth must be controlled among all the users those are provided through various communication systems, or the bandwidth will be wasted among the caller and called party and also may be wasted between the link and the end point (Medhi & Ramasamy, 2010).

By thinking of it a new algorithm is proposed. It is based on leaky Bucket algorithm with some specific features. This algorithm shapes the packets between the caller and the called party also between the link and the end point of the throughout the communication system. The packets are molded with the help of specific time buffer (Nakibly, 2014). The buckets are not static as normally as leaky algorithm uses. Increase number of packets the time delay is relatively less and the data's are optimized. The waste packets from the overflow data's are saved in an optimal bucket until the process of the previous step. Then the data's are sent sequentially. Overall Process ensures an optimization scheme within the whole network area.

3.1. Existing Technique for Bandwidth Optimization

There are many Bandwidth managing and optimizing options, they are listed below:
- **Traffic Shaping (Rate limiting):** Leaky bucket, Token bucket, TCP rate control- it adjusts the TCP window size as well as controlling the rate of ACK's being returned to the sender (Farzanegan Daneshvar, Saidi & Mahdavi, 2014).
  - o **Leaky Bucket Algorithm:** The Leaky Bucket Algorithm used to control data rate in a network. It is implemented as a single-server queue with constant service time. If the bucket (buffer) overflows, then packets are discarded (Rahman, 2019).
  - o **Token Bucket Algorithm:** The Token Bucket Algorithm allows the output rate to vary, depending on the size of the burst. In the Token Bucket algorithm, the bucket holds tokens. To transmit a packet, the host must capture and destroy one token. Tokens are generated by a clock at the rate of one token every Δt sec. Idle hosts can capture and save up tokens (up to the max. size of the bucket) in order to send larger bursts later (Farzaneh, Mardi & Ghorashi, 2014).
- **Scheduling Algorithms:** Weighted fair queuing (WFQ), queuing, Weighted (WRR), Deficit weighted round robin (DWRR), Hierarchical Fair Service Curve (HFSC) (Ash, 2006).
- **Congestion Avoidance:** RED, WRED works as port queuing buffer network scheduler and lowers the usual property of TCP global synchronization, Policing.
- **Bandwidth Reservation Protocols / Algorithms:** Resource reservation protocol (RSVP), Constraint-based Routing Label Distribution Protocol (CR-LDP), Top-nodes algorithm.
- **Traffic Classification:** Categorizing traffic according to some policy in order that the above techniques can be applied to each class of traffic differently (Dainotti, Pescape & Claffy, 2012).

4. PROPOSED ALGORITHM

Proposed algorithm is based on the "leaky bucket" algorithm. But it is very different than normal leaky bucket. As all know the leaky algorithm uses bucket which can contain both incoming and outgoing packets, shape them send them at a constant or optimal rate. But leaky algorithm uses fixed size of buckets and that cannot contain the overflow data as a result there are fall of packets. Being modified and changed the algorithm using FIFO queue as the number of queue equal to the no of buckets for traffic shaping (burst, noise) and processing the incoming packets then resend the overflow data through the next bucket fixing a time limit to transfer all the packets within a session and so on. The algorithm is effective for shaping the traffic, since all the packets are sent ensures relatively a smaller amount delay time provides effectiveness on channel capacity, also provides optimality with capacitive controlled bandwidth to a link and endpoint channel. Same work follows in case of caller and called party through data packet transferring.

There is a delay time for packet data intervals between links to end point packet transfer. It makes the delay time relatively less for this algorithm. So, it gives every time an optimal rate of packet transfer per second (Elhanany & Hamdi, 2007). For understanding the development, it is important to know about the time delay of a network system. So, for delay

Delay = F(Traffic volume data rate, Capacity)

For a single link system it assumes that packet arrival to a network link follows a Poisson process with the average arrival rate as 'λ' packets per sec. The average service rate of packets by the link is assumed to be 'μ' packets per sec (Medhi & Ramasamy, 2017). It considers here the case in which the average arrival rate is lower than the average service rate, if $\lambda < \mu$; otherwise, it would have an overflow situation (Ponomarenko, Kim & Melikov, 2010). If it assumes that the service time is exponentially distributed, in addition to packet arrival being Poissonian, then the average delay 'τ' can be given by the following formula, which is based on the M/M/1 queuing model.

$$\tau = \frac{1}{\mu - \lambda} \qquad (1)$$

Considering the average packet size is 'κ' Megabits, and that the packet size is exponentially distributed. Then, there is a simple relation between the link speed 'c' (in Mbps), the average packet size 'κ', and the packet service rate 'μ', which can be written as:

$$c = \kappa\mu \qquad (2)$$

Combining 'κ' with the packet arrival rate 'λ', it can consider the arrival rate 'h' in Mbps as follows:

$$h = \kappa\lambda \tag{3}$$

If multiply the numerator and the denominator by 'κ', it can then transform the above equations as

$$\tau = \frac{\kappa}{\kappa(\mu - \lambda)} = \frac{\kappa}{c - h} \tag{4}$$

The relation can be written as

$$\frac{\tau}{\kappa} = \frac{1}{c - h} \tag{5}$$

Now compare Eq. (1) and Eq. (2), t the average packet delay can be derived directly from the link speed and arrival rate given in a measure such as Mbps; the only difference is the factor 'κ', the average packet size. Considering the delay proposed algorithm stands the below equation:

$$\sum y = \sum X + \sum_{i=0}^{n} x \tag{6}$$

where: y – output rate, transfer/sec or packets/sec,
X – bucket size,
x – number of packets,
n – number of packets in serial through distribution.

Condition 1: if $X < x$, new bucket is generated, then equation stands as

$$y = X_1 + X_2 + \cdots + X_n + \sum_{i=0}^{n} x \tag{7}$$

where: X_1 – the previous bucket with stored packets,
X_2 – Overflow packets that will flow after the stored packets

Condition 2: if $X > x$, new bucket is not generated:

$$y = X_1 + \sum_{i=0}^{X} x \tag{8}$$

where: x – the optimal no packets sending through to the network.

Condition 3: If $X = 0$, in case of first bucket is empty.

Here, $X_1 = 0$ means, emptiness of packet or packets are being transferred successfully (Rahman, 2019; Rahman & Rahat Hasan Robi, 2019). Then fetish coming packets are added to the first bucket. Following above analogy this

algorithm performs less delay than both of the algorithms (leaky and token bucket). If 20 data packets are needed to be send with in a network this algorithm performs faster with a less delay time where leaky bucket and token bucket needs respectively more whether this algorithm needs a less time delay.
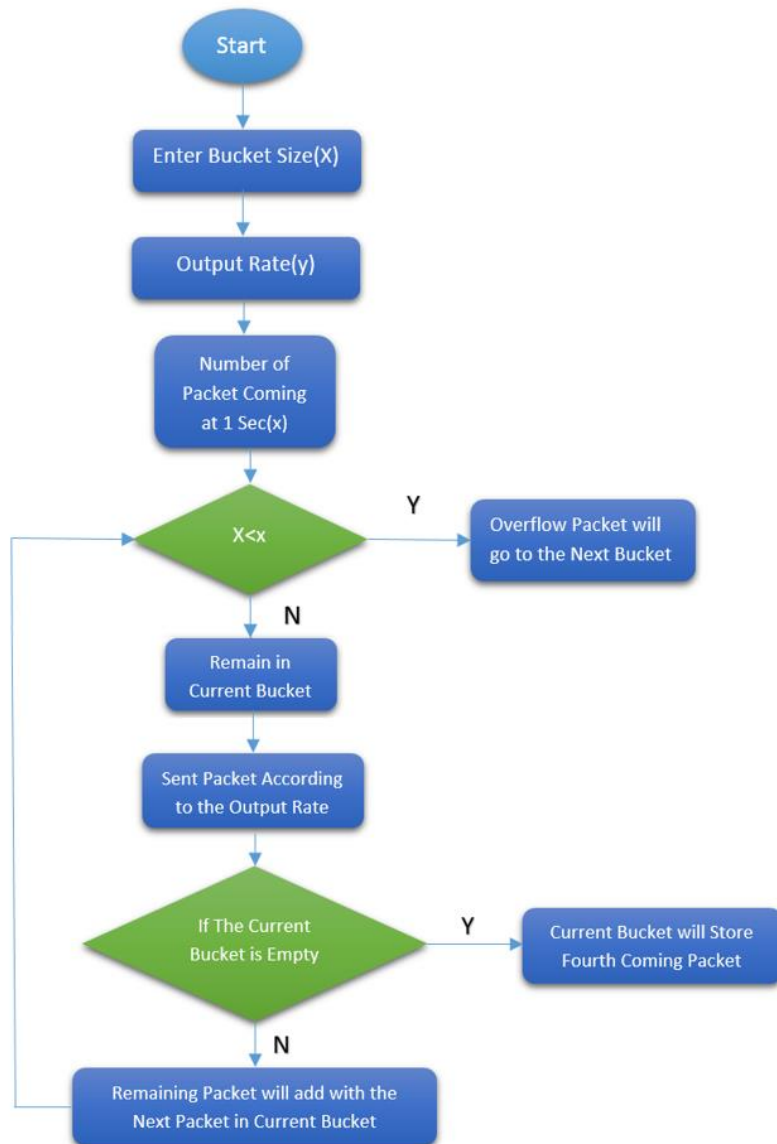

Fig. 2. Basic activity diagram of Proposed Algorithm
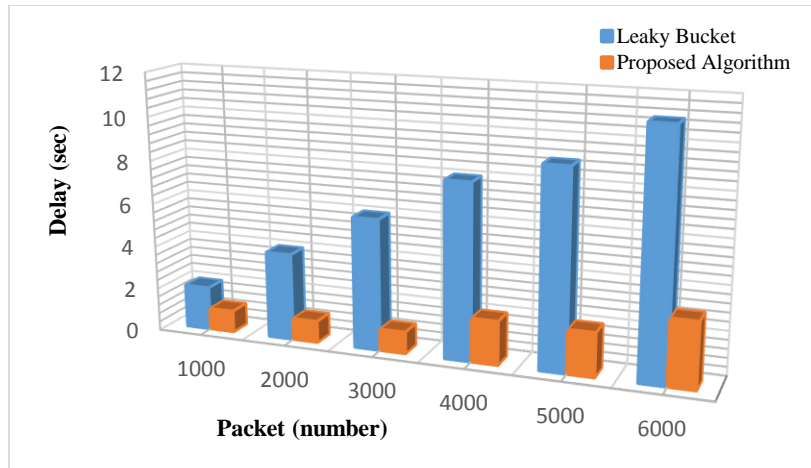
5. SIMULATION RESULTS

Fig. 3. Leaky Bucket vs. Proposed Algorithm (Delay)

Here leaky vs. proposed algorithm in terms of delay is shown in Figure 3. In the graph when 1000 packet send the delay is 2 second for Leaky bucket and 1 second for proposed algorithm. When 6000 packet send the delay is 11 second for Leaky bucket and 3 second for proposed algorithm. So, In Leaky bucket delay is increasing more than the proposed algorithm when the amount of packet is increased. That means less delay is happen in proposed algorithm.
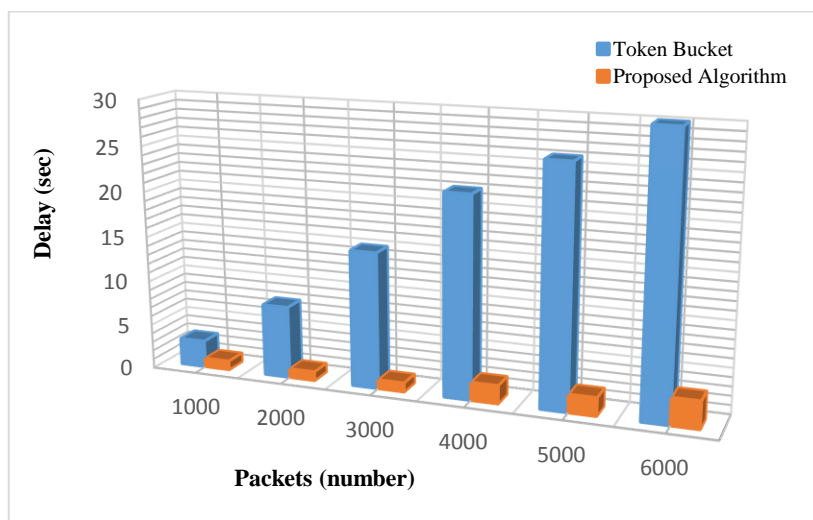

Fig. 4. Token Bucket vs. Proposed Algorithm (Delay)

49

Here Token vs. proposed algorithm in terms of delay is shown in Figure 4. In the graph when 1000 packet send the delay is 3 second for Token bucket and 1 second for proposed algorithm. When 6000 packet send the delay is 30 second for Token bucket and 3 second for proposed algorithm. So, In Token bucket delay is increasing more than the proposed algorithm when the amount of packet is increased. That means less delay is happen in proposed algorithm.
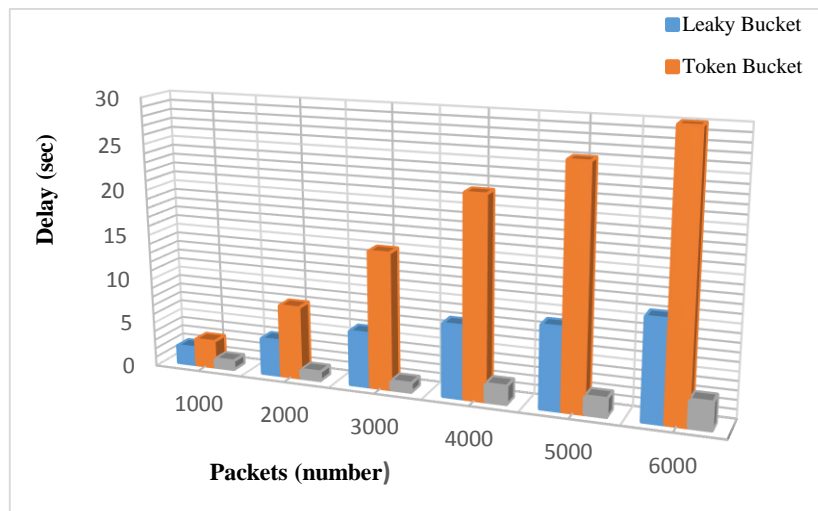

Fig. 5. Leaky Bucket vs. Token Bucket vs. Proposed Algorithm (Delay)

Here Leaky vs. Token vs. proposed algorithm in terms of delay is shown in Figure 5. Both Leaky and Token bucket make delay for sending packets. But whatever the amount of packets is sent the proposed algorithm make relatively less delay than Leaky and Token bucket.

Below performance comparison for 2000 Packets was showed.

Tab. 1. Performance Comparison

Performance (%)	Leaky Bucket	Token Bucket	Proposed Algorithm
Delay	2%	4%	0.55%

6. CONCLUSION

Mobile Ad Hoc Networks (MANET) provide one of the most emergent fields for research due to the high interest and it can offer in different sectors of our lives through the proper use of MANET. It is such an emerging technology that enables

a wide range of applications. To facilities' those services and applications the proposed bandwidth optimization technique used to provide an improved communication to optimize and enhanced the performance of MANET. In this research work, I have considered the bandwidth optimization technique in mobile ad hoc networks from the delay time viewpoint. I have analyzed various issue about bandwidth optimization and presented the design and analysis of a new bandwidth optimization technique for enhancement the performance of mobile ad hoc networks which is more efficient in terms of time delay and provides an optimal solution in an open and managed-open environment in Mobile Ad Hoc Network (MANET). The effectiveness of the proposed algorithm in terms of time delay in mobile ad hoc networks can redirect a new way towards optimization development in network communication. Comparing others, it can be said that the working process of the proposed scheme is far better. With a view to different measurements, the proposed new bandwidth optimization technique for mobile ad hoc network will be effective for pursuing an optimized platform.

REFERENCES

Siva Ram Murthy, C., & Manoj, B. S. (2004). *Ad Hoc Wireless Networks, Architecture and Protocols*. New York, USA: Prentice Hall PTR.

Basagni, S., Conti, M., Giordano, S., & Stojmenovic, I. (2003). *Mobile Ad Hoc Networks*. USA: IEEE Press, A john Wily & Sons, INC. Publication.

Aggelou, G. (2004). *Mobile Ad Hoc Networks. 2nd edition*. New York, USA: McGraw Hill professional engineering.

Agrawal, V. M., & Chauhan, H. (2015). An Overview of security issues in Mobile Ad hoc Networks. *International Journal of Computer Engineering and Sciences*, *1*(1), 9-17. doi:10.26472/ijces.v1i1.16

Perkins, Ch. E. (2008). *Ad hoc networking*. Harlow, England: Addison-Wesley Professional.

Pujolle, G. (2013). Metamorphic Networks. *Journal of Computing Science and Engineering*, *7*(3), 198-203. doi:0.5626/JCSE.2013.7.3.198

Medhi, D., & Ramasamy, K. (2010). *Network routing: algorithms, protocols, and architectures*. San Francisco, USA: Morgan Kaufmann.

Nakibly, G. (2014). *Traffic Engineering Algorithms for IP and MPLS Networks: Novel and practical algorithms for routing optimization of large operational networks*. Scholars Press.

Farzanegan Daneshvar, M., Saidi, H., & Mahdavi, M. (2014). A Scheduling Algorithm for Bursty Traffic: Controlling of Service Rate and Burst. *Arabian Journal for Science and Engineering*, *39*(6), 4753-4764. doi:10.1007/s13369-014-1086-7

Rahman, M. T. (2019). Enhancement of Inter-Vehicular Communication through a New Bandwidth Optimization Technique to Optimize the Performance of VANETs. *International Journal of Science and Research*, *8*(2), 966-971. doi:10.21275/ART20195166

Farzaneh, Y., Mardi, A., & Ghorashi, S. A. (2014). A QoS-aware downlink packet scheduler using token bucket algorithm for LTE systems. In *2014 22nd Iranian Conference on Electrical Engineering (ICEE)* (pp. 1775-1780). Tehran. doi:0.1109/IranianCEE.2014.6999826.

Ash, G. R. (2006). *Traffic Engineering and QoS Optimization of Integrated Voice and Data Networks*. Massachusetts, USA: Morgan Kaufmann.

Dainotti, A., Pescape, A., & Claffy, K. (2012). Issues and future directions in traffic classification. *IEEE Network: The Magazine of Global Internetworking*, *26*(1), 35-40. doi:10.1109/MNET.2012.6135854

Elhanany, I., & Hamdi, M. (2007). *High-performance packet switching architectures*. London, UK: Springer.

Medhi, D., & Ramasamy, K. (2017). *Network routing: algorithms, protocols, and architectures*. San Francisco, USA: Morgan Kaufmann.

Ponomarenko, L., Kim, Ch. S., & Melikov, A. (2010). *Performance analysis and optimization of multi-traffic on communication networks*. Heidelberg, Berlin: Springer. doi:10.1007/978-3-642-15458-4

Rahman, M. T., & Rahat Hasan Robi, F. M. (2019). Implementation of Secured Portable PABX System of Fully Fledged Mobility Management for Unified Communication. *International Journal of Engineering Research and Advanced Technology*, *5*(2), 80-92. doi:10.31695/IJERAT.2019.3389

Kusay F. AL-TABATABAIE [0000-0002-6632-3596]*,
*Sadeer D. ABDULAMEER**

APPLYING ARDUINO FOR CONTROLLING CAR PARKING SYSTEM

Abstract

With increasing automobiles in the parking space, we could face problems like unplanned parking, lack of discipline, wasting time and fuel while looking for free space around the parking ground. These problems could be solved by applying Arduino for controlling car parking system. The proposed system will detect an available parking slot in short time, saves fuel, offer monitoring car parking system with low consumption, easy to implement and inexpensive.

1. INTRODUCTION

An important factor which leads to a parking problem is human behavior. Due to time deviation in arrival rate, habitual parking lots cannot be concerned with the user. So, the users indiscriminately park the car in a parking space, and some do not have space, and they park outside of parking space.

Fully automated systems are being adopted in industries across the world at a rapid rate (Al-Tabatabaie & Hama, 2017). Control systems are replacing manual operators and fully automated machines are replacing human labor. Less personnel and smarter machines mean less operating and labor costs while increasing the quality of the products or services offered.

This study will increase the quality of service of parking lots by integrating a smart system which assists motorists in finding vacant parking slots (Bonde, Shende, Kedari, Gaikwad & Bokre, 2014). It will provide system with information to assist in monitoring the vehicles safely.

---

* Cihan University – Sulaimanyia Campus, Computer Science Departament, Sulaimanyia, Iraq, kusyt@yahoo.com, kusay.faisal@sulicihan.edu.krd, sadeer.alatter@gmail.com

Arduino will be used as a controller to the system, Arduino is an open-source prototyping platform based on easy-to-use hardware and software (Official Arduino website), support allows external USB hardware (an Android USB accessory) to cooperate with an Android-powered device in a special accessory mode. When an Android-powered device is in accessory mode, the connected accessory acts as the USB host (powers the bus and enumerates devices) and the Android-powered device acts in the USB accessory role. The accessory mode is ultimately dependent on the device's hardware and not all devices support accessory mode (Official Arduino website).

Recently there are a number of researches have been done for car parking using Arduino with different ideas like using Internet of things (IOT) technology (Ghosh, Prusty & Natarajan, 2018; Kadhim, 2018; Yuvaraju & Monika, 2017), some researchers used fuzzy design (Ganesh, Deepak, Naveen & Raghu, 2014; Rashid, Rahman, Islam, Alwahedy & Abdullahi, 2019; Syam, Piarah & Jaelani, 2015), and some researchers used image processing (Al-Kharusi & Al-Bahadly, 2014; Mallikarjun, Harikishan, Sharath & Rakesh, 2019), while others use it with GSM module using mobile (Ba Sabbea et al., 2018; Rahayu & Mustapa, 2013; Ramani, Valarmathy, Vanitha & Thangam, 2013). The intelligent or smart parking system must be proposed for searching the vacant or about to vacant parking space (Aalsalem, Khan & Dhabba, 2015). In smart parking system, users can access data to determine the availability of spots for parking, then have card notify the entrance time, at the exit, there will be a small pad to type in the card number to check how much money have to pay before opening exit gate. Thus, smart parking will increase the application of existing parking, which leads to greater income for parking holders. It also benefits the environment and plays a major role in creating an eco-friendly environment.

2. THE INSTALLMENT SYSTEM

To have proper knowledge about the hardware components as well as the software components of the project is a must. Arduino Mega 2560 played a vital part in this project as it contains all the software data in it. The required hardware components for the project are:

2.1. Arduino Mega 2560

The Arduino Mega is a microcontroller board based on the ATmega2560. The ATmega2560 is a low-power CMOS 8-bit microcontroller based on the AVR enhanced RISC architecture. By executing powerful instructions in a single clock cycle, the ATmega2560 achieves throughputs approaching 1 Minute Per Second per MHz allowing the system design to optimize power consumption versus processing speed (Al-Tabatabaie & Hama, 2017; Official Arduino website) . The Mega 2560 is as shown in figure 1.

Fig. 1. Arduino Mega 2560 board

Where figure 1 shows all pins outputs digital, analog, power and ground, details as shown in table 1.

Tab. 1. Technical specification for Arduino Mega 2560

Microcontroller	ATmega2560
Operating Voltage	5V
Input Voltage (recommended)	7–12V
Input Voltage (limit)	6–20V
Digital I/O Pins	54 (of which 15 provide PWM output)
Analog Input Pins	16
DC Current per I/O Pin	20 mA
DC Current for 3.3V Pin	50 mA
Flash Memory	256 KB of which 8 KB used by boot-loader
SRAM	8 KB
EEPROM	4 KB
Clock Speed	16 MHz
Length	101.52 mm
Width	53.3 mm
Weight	37 g

2.2. RF Module (radio frequency module)

Is a small electronic device used to transmit and/or receive radio signals, as shown in figure 2. This post is popular to monitor RF for frequency of 433MHz Transmitter/Receiver modules with Arduino.
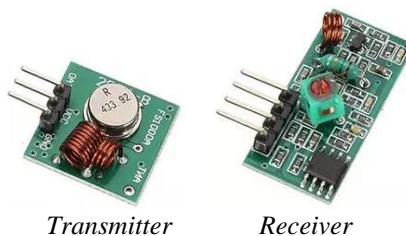

Transmitter   *Receiver*

Fig. 2. RF "Transmitter/Receiver module"

2.3. L293D motor driver

H-bridge is an electronic circuit that enables a voltage to be applied across a load in either direction as shown in Figure 3.
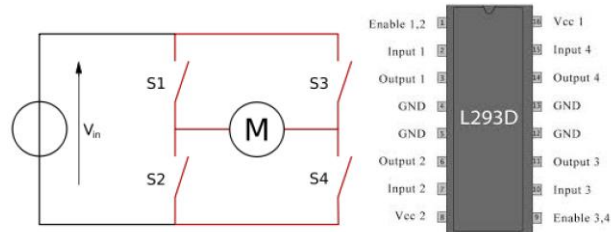

Fig. 3. L293D motor driver module

These circuits are often used to allow DC motors to run forwards or backward in robotics and other applications.

2.4. DC Motor

Is a rotary electrical machine, the most common types rely on the forces produced by magnetic fields as shown in figure 4.
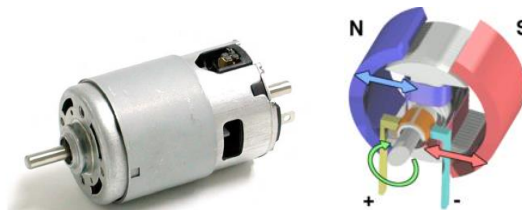

Fig. 4. DC step motor

The DC motor converts from direct current electrical energy into mechanical energy.

2.5. Ultrasonic sensor

Is Range Detection Sensor to indicate the empty slot in the garage, as shown in figure 5.
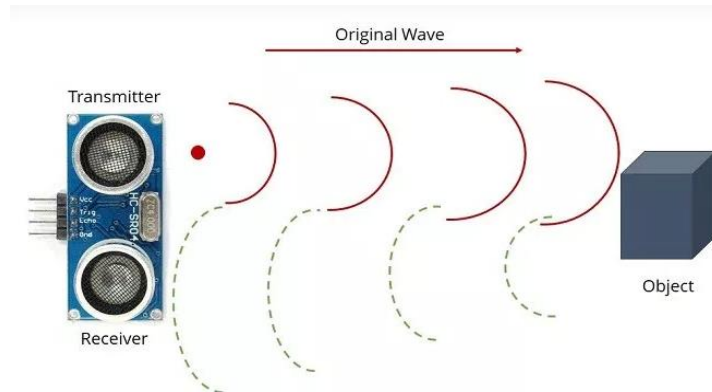
Fig. 5. Ultrasonic range detection

By measuring the distance to find the empty slot in parking to park the car and help the driver to find the slot easily. The ultrasonic sensor determines the distance to an object by using sonar. Here's what happens:

1. The transmitter (trig pin) sends a signal: a high-frequency sound.
2. When the signal finds an object, it is reflected and…
3. The transmitter (echo pin) receives it.

3. METHODOLOGY

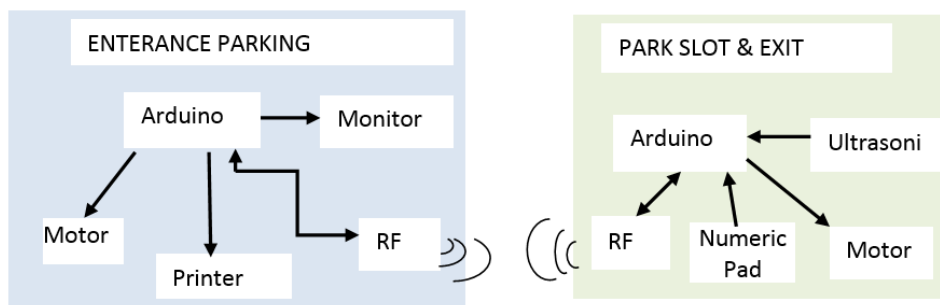The proposed system architecture idea present as shown in Figure 6.

Fig. 6. System architecture idea

The methodology of Automated Car Parking System is made up of 2 major components: Arduino Mega 2560 and RF Module. The coding of this system has been done using the ArduinoIDE programming language. The monitor will display the number of available slots and will have an RF Receiver Module to get updates about the empty parking slot.

When a car will come, the operator will send an instruction through Arduino to open the gate using RF Transmitter Module, the ultrasonic will sense which slot number car barked and through Arduino will update the monitor display at the entrance. DC motor helps the gates to open up when it gets the signal from Arduino, Arduino will only get the signal to DC motor using RF Receiver Module. The timer will be started as soon as the gate opened. The operator will print slot number, time and the code number in the small paper for the driver to take it. The code number will be saved in the system against a slot number.

For parking out the user must make payment to be provided with a code to the operator at the exit gate. After the user makes payment must type the code number at the numeric pad at the gate to let the operator giving the command to park out the car. The operator will update the empty slot information to the monitor display at the entrance using the RF Transmitter Module. The block diagram for the park system is shown in Figure 7.
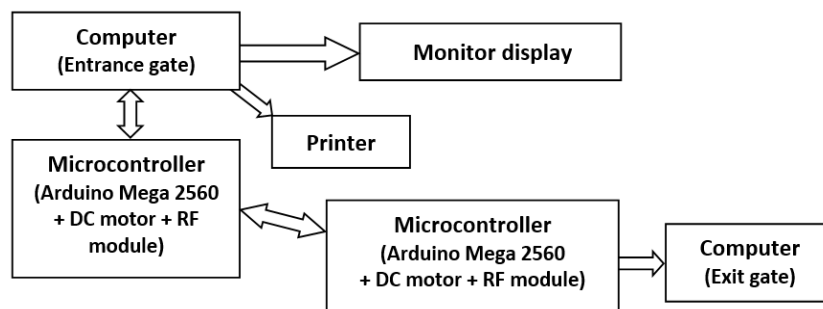

Fig. 7. Prototype block diagram for automated car parking system

4. WORKING PROCEDURE

This section will explain the working procedure for the prototype block diagram in Figure 7 at the computers in the entrance and exit gates. That would be done by simplifying the work using flowcharts.

4.1. Computer (Entrance Gate)

The monitor will display the available free slots where the user can park, the calculation would be saved in the computer as follows:

Total slot = n; Busy Slot = a;
After every entry:
a = a + 1; Free Slot = n − a;

58

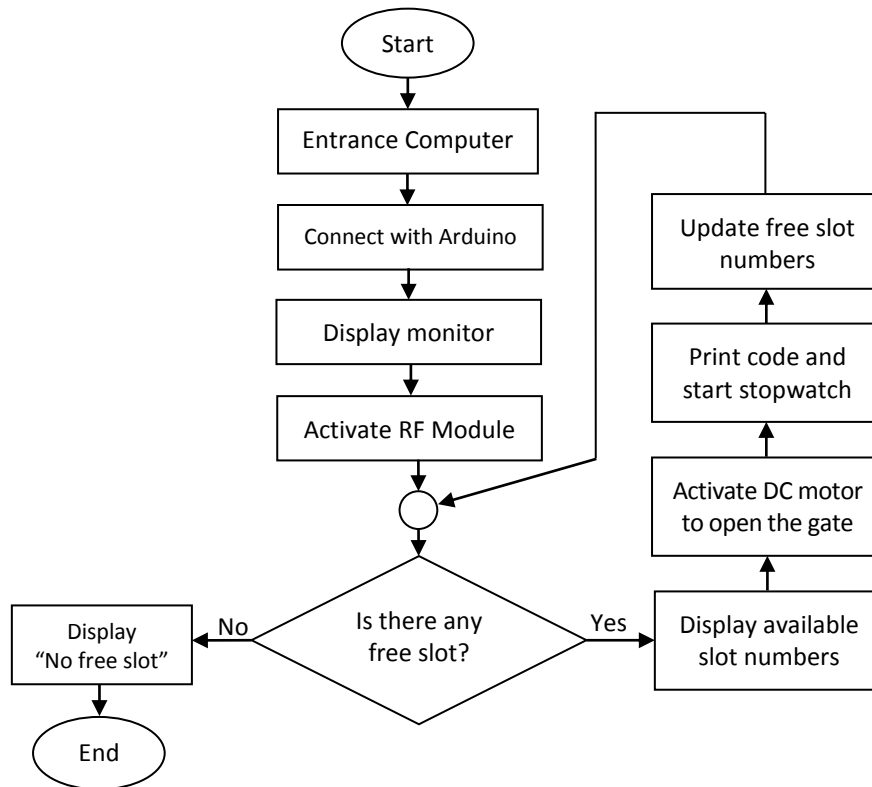The flowchart for the entrance computer is shown in figure 8.

Fig. 8. Flowchart for the entrance gate

4.2. Pricing principle and time limit

The pricing principle and time limit for automated car parking system will be saved inside the computer database, the customer should put the ticket inside the machine to check how long stayed and gives how much have to pay. This time as shown in table 2 given below:

Tab. 2. Time limitation plan for car parking system

Place name	Time limit (hours)	Price per hour (in USD)
Shopping Mall	3	1.25
Amusement Park	4	1
Hospitals	2	0.5
Office space	Office hours	Free for worker only

As shown in table 2, plan for each place required to apply the Arduino system with a price to pay for each time limitation, where the price will be the number of exceeding the time limit. For example, the price is 1.25 USD for parking 3 hours in the shopping mall and it would be 2.5 USD if exceeded 3 hours. However, it would be 3.75 USD if exceeded 6 hours. The same process would be applied to other places.

4.3. Computer (Exit Gate)

The ultrasonic will record in the map any available slot and update the computer, the gate will not open unless money has been paid, type in the code using numeric pad to activate Dc motor to open the gate as shown in figure 9.
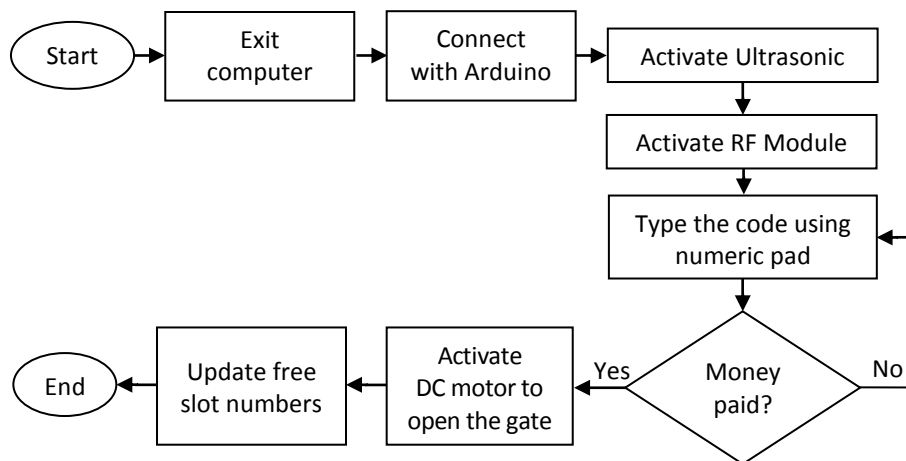

Fig. 9. Flowchart for the exit gate

5. EXPERIMENTAL RESULTS

The CPS (Car Parking system) has been tested and verified for the required results. The CPS is able to carry out the prime functionality of searching for an empty parking slot and communicate that path to the car. For data analysis and results, it has been compared between the normal car parking and CPS prototype by calculating savings and fuel consumption. The approximate calculations were as shown in table 3.

Thus, the proposed system relatively is higher than it is in the existing systems. From the experiment, results shows that when car numbers increases, will cause to reduce the detection accuracy. The reduction in accuracy was due to installing one ultrasonic sensor for every three slots. To maximize the accuracy of the proposed system suggest the installation of 1 sensor per parking slot. Thus, for each slot, the accuracy of detection is 100%.

Tab. 3. Approximate calculations of experimental results

Parameters of comparison	Normal car parking	Car Parking system
Space needed per slot (ft)	15/8	15/8
Maintenance cost per month (USD)	200	87.5
Staff needed at the parking	5	2
Detection of empty slot	Have to search manual	Use IR & Ultrasonic sensor
Parking method	Manual	Path tracking
Fuel consumed per hour per 100 km (liter)	2	1.4
Average distance traveled by a car to park in or park out (km)	46.11	38.7
Fuel consumed per car to park in or park out a car (litre)	0.276	0.085
Average time needed to park in or park out a car (minutes)	7.5	2.5
Average time to wait in a queue (minutes)	5–10	1.5
Time saved (minutes)	6	1

6. CONCLUSIONS

After applying the CPS it is found that the system can be introduced and will be beneficiary for many countries. The main benefits are time and fuel saving, it is also providing sustainable parking in an eco-friendly manner. There is less maintenance cost for this system so it helps the property developer in cost saving, and reduces the traffic jam. It will help the developers to increase their income as well as it helps the government by increasing tax revenue. Therefore we should introduce CPS and enjoy the benefits.

7. FUTURE ENHANCEMENT

It is possible to enhance the system by including different applications, such as internet booking by utilizing GSM, where the driver can book for the parking area at home or while in transit to the shopping center. Also, it is possible to include image processing to the system to recognize the cars by their number plates, by using this type of technology users can directly pay the car parking using a mobile phone.

REFEERENCES

Aalsalem, M. Y., Khan W. Z., & Dhabba, K. M. (2015). An automated vehicle parking management and monitoring system using ANPR cameras. In *IEEE 17th International Conference on Advanced Communication Technology (ICACT)* (pp.706–710). Seoul, South Korea.

Al-Kharusi, H., & Al-Bahadly, I. (2014). Intelligent Parking Management System Based on Image Processing. *World Journal of Engineering and Technology*, *2*, 55–67. doi:10.4236/wjet.2014.22006

Al-Tabatabaie, K. F., & Hama, K. D. (2017). Remote Automation System Control Using Arduino Board. *International Journal of Latest Trends in Engineering and Technology (IJLTET)*, *8*(3), 161–167. doi:10.21172/1.83.022

Ba Sabbea, M. O., Irfan, M., ALtamimi, S. K., Saeed, S. M., Almawgani, A. H. M., & Alghamdi, H. (2018). Design and Development of a Smart Parking System. *Journal of Automation and Control Engineering, 6*(2), 66–69.

Bonde, D. J., Shende, R. S., Kedari, A. S., Gaikwad, K. S., & Bokre, A. U. (2014). Automated Car parking system commanded by android application. In *IEEE International Conference on Computer Communication and Informatics* (pp. 1–4). Coimbatore, India.

Ganesh, S., Deepak, S., Naveen, B. M., & Raghu, S. (2014). Fuzzy Based Design of Parallel Park Assist System Control Strategy. *International Journal of Innovative Research in Computer Science & Technology (IJIRCST)*, *2*(6), 87–95.

Ghosh, S. K., Prusty, S., & Natarajan, P. B. (2018). Design and Implementation of Smart Car Parking System Using Lab VIEW. *International Journal of Pure and Applied Mathematics, 120*(6), 329–338.

Kadhim, M. H. (2018). Arduino Smart Parking Manage System based on Ultrasonic Internet of Things (IoT) Technologies. *International Journal of Engineering & Technology*, *7*, 494–501.

Mallikarjun, G. H., Harikishan, B. H., Sharath, N., & Rakesh, M. (2019). Low Cost Arduino Based Smart Parking Lot Controller with Occupancy Counter. *International Journal Adance Scence Engineering*, *5*(3), 1027–1031. doi:10.29294/IJASE.5.3.2019.1027-1031

Rahayu, Y., & Mustapa, F. N. (2013). A Secure Parking Reservation System Using GSM Technology. *International Journal of Computer and Communication Engineering*, *2*(4), 518–520. doi:10.7763/IJCCE.2013.V2.239

Ramani, R., Valarmathy, S., Vanitha, N. S., & Thangam, R. (2013). Vehicle Tracking and Locking System Based on GSM and GPS. *I.J. Intelligent Systems and Applications*, *9*, 86–93. doi:10.5815/ijisa.2013.09.10

Rashid, M. M., Rahman, M. M., Islam, M. R., Alwahedy, O. N., & Abdullahi, A. (2019). Autonomous 4WD Smart Car Parallel Self-Parking System by Using Fuzzy Logic Controller. *American International Journal of Sciences and Engineering Research*, *2*(2), 1–31.

Syam, R., Piarah, W. H., & Jaelani, B. (2015). Controlling Smart Green House Using Fuzzy Logic Method. *International Journal on Smart Material and Mechatronics IJSMM, 2*(2), 116–120. doi:10.20342/IJSMM.2.2.116

Yuvaraju, M., & Monika, M. (2017). IOT Based Vehicle Parking Place Detection Using Arduino. *International Journal of Engineering Sciences & Research Technology (IJESRT)*, *6*(5), 536–542. doi:10.5281/zenodo.375816

Isaac FLORES-HERNÁNDEZ [0000-0003-4620-9144]*,
Edmundo BONILLA-HUERTA [0000-0003-2062-4219]*,
Perfecto Malaquías Quintero-Flores*, Oscar Atriano PONCE**
José Crispín HERNÁNDEZ-HERNÁNDEZ*,

APPLYING INTELLIGENT TECHNIQUES FOR TALENT RECRUITMENT

Abstract

The objective of this research is to describe a system to aligned the hard and soft skills of the applicant to the current labor market. For this, a system was implemented which uses Web Scraping to get a general profile of an area, meanwhile for the evaluation of the applicant soft skills is used a Test Cleaver and for the hard skills fuzzy inference system is implemented. Therefore, the data is entered into an Analytic Hierarchy Process, with this, the applier is able to see which area is better to improve according to the hard and soft skills.

1. INTRODUCTION

The profile of graduates of the universities in the different sectors of industry and research worldwide are evolving and frequently changing. Therefore, the skills that are expected from them are more technical and specialize. This make cause that many of the vacant posts to not be fill in many different areas, which leads to the increase of the unemployment index in Mexico. From the employer point of view the selection process is very important but takes a lot of time and human resources for the evaluation filters and the hiring of the appropriate candidate for a specific position, this reveals a flaw in the communication between the universities and the industries on the development of the skills that the graduates require in the work sector.

---

* Instituto Tecnológico de Apizaco, Computer Systems Department, Fco I Madero, Barrio de San José, 90300 Apizaco, Tlaxcala, México, isaac_camus@hotmail.com, edbonn@walla.com, malakaz_81@hotmail.com, josechh@yahoo.com.
** Smartsoft America BA, Calle Adolfo López Mateos, Texcacoac, 90806 Chiautempan, México, oatriano@smartsoftamerica.com.mx

In order to solve this problem, several methodologies had been applied for instance: the decisional tree J48 and random forest (Algur, Bhat & Kulkarni, 2016), which are used in order to predict if a student will be admitted depending on factors such as: Average aggregate score of all the semesters in CGPA, Communication Skill, Placement Preparation Hours per Week, Breaks between 12th and Engineering in Years, Performance in Extra Curricular Activities, Performance in Cultural Activities, Number of Industrial Visits during the course.

In his paper (Koutra, Kardaras, Barbounaki & Stalidis, 2017) use the Analytic Hierarchy Process (AHP) method incoperation with the Correspondence Analysis (CA), by doing this forms qualitative evaluations scales based on the data without any previous supposition.

In the other hand, (Rianto, Budiyanto, Setyohadi & Suyoto, 2017) designed an evaluation model using different criteria and sub-criteria, the weights of each one of this indicator was achieved through AHP, and then the range of alternatives of the student selection is calculated using TOPSIS. The considering criteria where: Academic ability, English Ability, Psycho test, Attitude, Soft Skill, Communication skills, Solve problems and think critically, Time management, Teamwork, Flexible & Adaptation.

In this paper a system based on Fuzzy Logic is proposed, Web Scraping and AHP (Analytic Hierarchy Process) to match the formation of the graduates with the demands of the industry.

2. METHODOLOGY

2.1. Test cleaver

The test cleaver is used by many Mexican companies for the recruiting and selection process of the personnel. It was designed in 1959 in Princeton New Jersey by J.P Cleaver & CO (Gil-Gaytán & Núñez-Partido, 2017). It is a specific technique to respond to the personnel selection needs, the main objective of this technique is to measure the work conduct to be able to place the appropriate person for the appropriate job. It is because this technique measures the behavior and skills of the evaluated candidate, this is because it provides a description of the natural and daily conduct of an individual at work, which allows to determine if the candidate possess the ideal work skills for a position or the ability to perform properly in a specific area.

2.2. Fuzzy Logic

Fuzzy logic was introduce in 1965 by Lofti A Zadeh in his paper "fuzzy sets" (Zadeh, 1965) which presented a way to process the information in a way that the data can have a partial membership degree associated to different sets, stating the fuzzy sets theory.

The fuzzy sets allow to formalize linguistic excretions that have some ambiguity degree, in other words, provides a method to mathematically express concepts like: tall, cold, fast. Etcetera; that in everyday life are used consistently, but are not precise in themselves, this is why the membership degree of an element to a set is determined by a membership function that may contain all the real values between the interval [0,1]. The formal definition of a fuzzy set is:

A fuzzy set A in X is expressed as a set of ordered pairs:

$$A:\{x, \mu_A(x) \mid x \in X\},\qquad(1)$$

where: A – Represent the Fuzzy Set,
$\mu_A(x)$ – Represent the Membership Function,
$x \in X$ – Universe of universe of discourse.

Thus a fuzzy set is totally characterized by the membership function (MF) that indicates the degree in which every element of the universe belong to a given universe. There are many membership functions but the commonly used are Triangular MF, Trapezoidal MF and the Gaussian MF.

The Fuzzy rules are conditional sentences shape as IF-THEN, where de fuzzy propositions of the premises are related with the consequent by the implication, for example:

IF x is A THEN y is B

Where A and B are linguistic values defined by fuzzy sets in the universe X and Y. The (IF x is A) part is called premise or antecedent, meanwhile the (THEN y is B) part is called consequent or conclusion. For example

IF road is wet THEN driving is dangerous

In the classic rules systems, if the premise is true then the consequent is true. In the fuzzy systems this is different, because the premise is fuzzy variable, this why the rules are partially executed, therefore the consequent is true in a certain degree.

A fuzzy logic system used the inference like a calculus mechanism for a system where the input and output are numbers. A basic inference system is composed by 5 elements:
- Set of rules IF-THEN,
- A data base,
- Decision-making unit,
- Fuzzification unit,
- Defuzzification unit.

One of the most used inference systems methods based in linguistic rules was proposed in 1975 (Mamdani & Assilan, 1975), in an attempt to try to control a combination of the steam motor and boiler by a set of rules. This process has 4 steps:

- − Fuzzification of input variables: Consist on taking the crisp values of the input and determine the membership degree to the fuzzy sets associated.
- − Evaluation of the rules: Takes as the input the fuzzified values and it applied to the premises in the fuzzy rules. If a rule has multiple premises the operator And/Or are used to get only one number that represent the evaluation and its applied to the conclusion.
- − Aggregation of the output rules: Is a unification process of the output of all the rules, which means the membership function of all the consequents are combined (By union) to get and only fuzzy set for each output variable.
- − Defuzzification: Is the final result usually expressed by a crisp value.

2.3. Web Scraping

Data mining is currently a powerfull tool, because is one way to get information form a set of data (Broucke & Baesens, 2018). A part of the data mining is web content mining which has 4 extraction ways:

- − Not structured Data mining,
- − Structured Data mining,
- − Semi-structured Data mining,
- − Multimedia data extraction.

Web Scraping is a technique which is part of not structured Data mining, which consist in the extraction of one or many web pages from a same site, to manipulate, process and analyze part of its content.

2.4. Analytic Hierarchy Process

The Analytic Hierarchy Process was developed in 1980 by Thomas L. Saaty (Saaty, 1980). Is a multicriterial method that provides an evaluation for the alternatives to problems that contain multiple criteria, depending on the relative importance of each one of them, and then specifies the preference according to each one of the decision alternatives for each criteria. The result is the establishment of a hierarchy according to the priorities that shows the global preference for each one of the decision options. Is a worldwide use process in a wide variety if situation on different fields such as, health, business, government, education, etc.

3. IMPLEMENTATION

The proposed model is composed by 3 parts that are shown (figure 1).
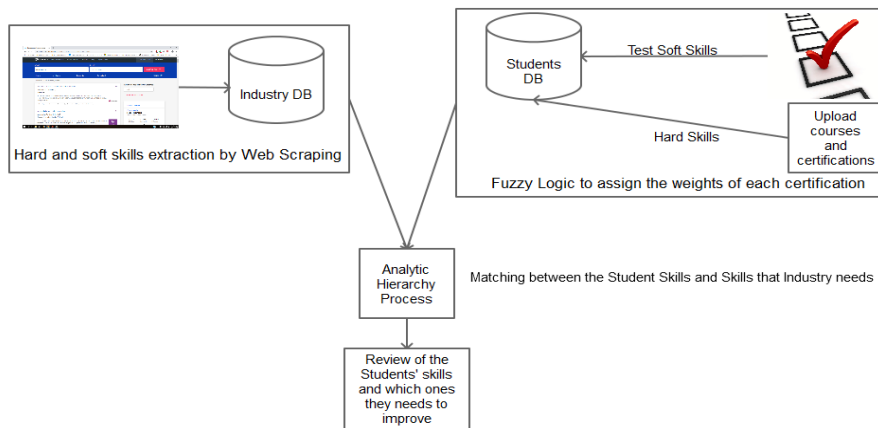

Fig. 1. Proposed System

The first part implemented was the web scraping in order to extract the hard and soft skills from job offers. To be able to do this the web site for the data mining was selected: OCCMundial (www.occ.com.mx) thus the web page structure had to be thoroughly analyzed for the purpose of obtaining the data to be extracted.

Once the design analysis was done it was determined to extract all the text referring to the job offer and the search the hard and soft skills required in the job market was done using previously elaborated dictionaries. The design of the dictionary for the soft skills was done taking into account the different writing styles for these offers, this is because the verbs can be conjugated in different indicative tenses in Spanish, which makes the search more difficult. To solve this issue the use of regular expressions was required in a way that the base form of the verb was looked for without caring the indicative tense used. 29 soft skills were considered which can be seen in table 1.

Tab. 1. Soft Skills

responsib[\w]	stress|work under pressure	positi[\w]
organiz[\w]	commit[\w]	initiative
tolera[\w]	interest*[\w]	flexib[\w]
analy[\w]	sincer[\w]	honest*[\w]
teamwork	adaptab[\w]	punctual*[\w]
collaborat[\w]	enthusias[\w]	critical
[\w]*active|proactivity	reliable | confidence	socia[\w]
availab[\w]	integrity | honest person	dedicat[\w]
attitude	patien[\w]	assertive*[\w]
communication | easy word	decisive	

For the hard skills this process was easier, because of the lack of conjugation of the word use, the 20 hard skills can be seen in table 2.

Tab. 2. Hard Skills

java	html 5
.net	css
visual studio	jquery
asp	boostrap
php	sql
javascript	mvc
sql server	rest
postgresql	ajax
json	ios
c sharp|c#	android

Once the results had been obtained are analyze, and as a result we get a general profile for certain specific job, for instance what are the skills that a programmer needs according to the requirements in the working market.
For examples, the soft skills more sought for a programmer are:
– Teamwork,
– Adaptable,
– Responsible,
– Integrity,
– Analytical.
The hard skills more require for a programmer are:
– iOS,
– SQL,
– Java,
– REST.
– .Net.

The second part is address to the evaluation of soft and hard skills of the applier. To evaluate soft skills a psychological test designed under the Cleaver Model was used, providing a description of the applier emphasizing the skills. The skills to be evaluated in the test match the ones in the dictionary of the first stage in the system see (Fig. 1), and the interface can be seen in figure 2.

Fig. 2. Interface of Test Cleaver

The evaluation of the hard skills is done when the applier tape in the data about certifications and current courses. This data is entered into a fuzzy inference system, which stablishes if the hard skill is good enough. An example of the interface can be seen in figure 3:

Fig. 3. Interface of System Fuzzy

Where the area of certification is selected by the user selects the certification area (Programing, Network and DataBases), the beginning and the end of the certification course; and finally the company or institution that gave it.

Once the data had been entered this are arranged in the 2 fuzzy sets proposed, the first one regarding the certification time, for this purpose 3 linguistic variables are considered, which can be seen in figure 4.

Fig. 4. Validation Fuzzy Set

The second fuzzy set is a singleton according to the certifying company, which have a value of 1 (Google, Amazon, Microsoft, IBM, Cisco, ITIL, ISACA), 0.75 (CompTIA, PSP) y 0.25(Other companies). That can be seen in the figure 5.
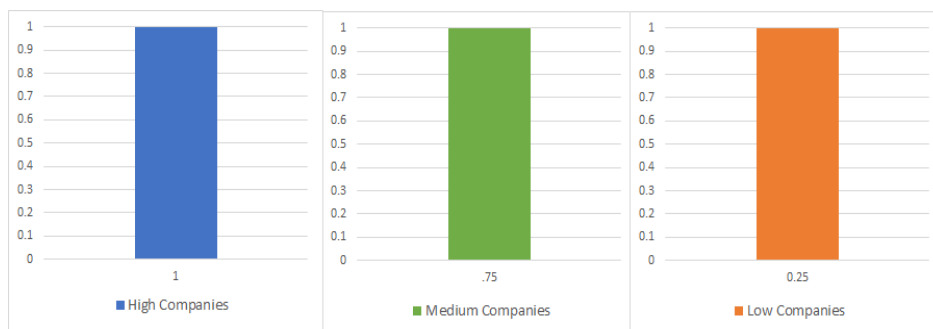
Fig. 5. Singleton Fuzzy Set

In this way for the 2 inputs (Months, Company) membership degree to the fuzzy sets is determined and associated. Immediately after this, the fuzzified data is enter in the 9 previously designed fuzzy rules, which are:

- IF validation = Excellent and company = High THEN Hard_skill = High,
- IF validation = Excellent and company = Medium THEN Hard_skill = Medium,
- IF validation = Excellent and company = Low THEN Hard_skill = Medium,
- IF validation = Good and company = High THEN Hard_skill = High,
- IF validation = Good and company = Medium THEN Hard_skill = Medium,
- IF validation = Good and company = Low THEN Hard_skill = Low,
- IF validation = Average and company = High THEN Hard_skill = Medium,
- IF validation = Average and company = Medium THEN Hard_skill = Low,
- IF validation = Average and company = Low THEN Hard_skill = Low.

After the activation of the corresponding rules, the aggregation of the selected output is done, this means to make a combination of the membership function of all the consequents of the rules to get a unique fuzzy set for each output variable. The final result is shown by a crisp value which represent the hard skill of the applier.

Having obtained this data is enter to AHP to obtain a comparison between the applier skills and the skills that the market requires. An example of this is shown in figure 6.

Fig. 6. Data obtained entered into the AHP

Through this process the applier is able to see which area is more appropriated according to the hard and soft skills displayed, most importantly it will show which skills the applier needs to improve according to the current work market.

71

4. CONCLUSIONS

According to this, the set of methodologies implemented in the proposed system is considered a good alternative, because it's possible to guide an 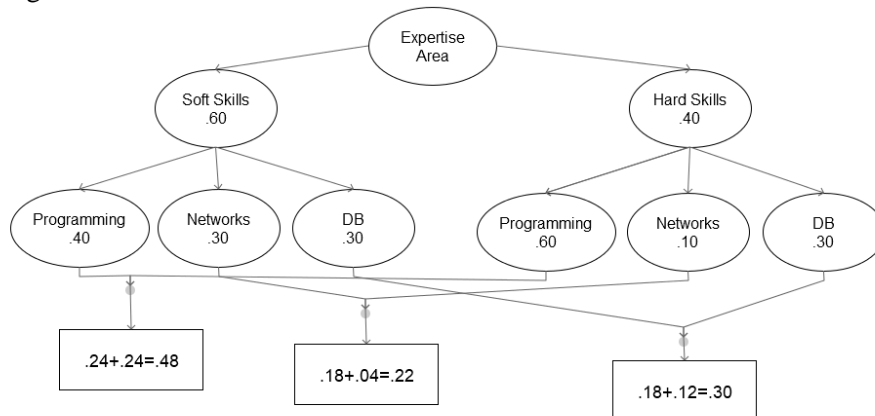applicant to the requirements of the labor market considering their soft and hard skills, this helps to the applicant to know their weaknesses and in which skills are better. Besides the implemented methodologies complement each other in order to do this type of evaluation; The web Scraping help to create the general profile, while the Test Cleaver and Inference Fuzzy System help to know the applicant skills. Thus, with the data, the applicant is evaluated by AHP according to the current work market.

Therefore, the system fulfills its purpose, which is given to the applicant a profile considering their soft and hard skills according to the current labor market.

REFERENCES

Algur, S., Bhat, P., & Kulkarni, N. (2016). Educational Data Mining: Classification Techniques for Recruitment Analysis. *International Journal of Modern Education and Computer Science (IJMECS)*, *8*(2), 59–65. doi:10.5815/ijmecs.2016.02.08

Broucke, S., & Baesens, B. (2018). *Practical Web Scraping for Data Science: Best practices and Examples with Python*. New York: Apress. doi: 10.1007/978-1-4842-3582-9

Gil-Gaytán, O. L., & Núñez-Partido, A. (2017). Rasgos de personalidad de exportadores mexicanos con éxito. *Revista Academia & Negocios*, *3*(1), 23–34.

Koutra, G., Barbounaki, S., Kardaras, D., & Stalidis, G. (2017). A multicriteria model for Personnel selection in Maritime Industry in Greece. In *2017 IEEE 19th Conference on Business Informatics* (CBI) (pp. 287–294). Thessaloniki. doi:10.1109/CBI.2017.52

Mamdani, E. H., & Assilan, S. (1975). An Experiment in Linguistic Synthesis with a Fuzzy Logic Controller. *International Journal of Man-Machine Studies*, *7*(1), 1–13. doi:10.1016/S0020-7373(75)80002-2

Rianto, Budiyanto, D., Setyohadi, & Suyoto. (2017). AHP-TOPSIS on Selection of New University Students and the Prediction of Future Employment. In *2017 1st International Conference on Informatics and Computational Sciences (ICICoS)* (pp. 125–130). Semarang. doi: 10.1109/ICICOS.2017.8276349

Saaty, T. L. (1980). *The Analytic Hierarchy Process*. New York: McGraw-Hill.

Zadeh, L. A. (1965). Fuzzy sets. *Information and Control*, *8*(3), 338–353. doi:10.1016/S0019-9958(65)90241-X

Rosa Maria VAZQUEZ[*], Edmundo BONILLA[*],
Eduardo SANCHEZ[*], Oscar ATRIANO[**], Cinthya BERRUECOS[**]

APPLICATION OF DATA MINING TECHNIQUES TO FIND RELATIONSHIPS BETWEEN THE DISHES OFFERED BY A RESTAURANT FOR THE ELABORATION OF COMBOS BASED ON THE PREFERENCES OF THE DINERS

Abstract

Currently, blended food has been a common menu item in fast food restaurants. The sales of the fast-food industry grow thanks to several sales strategies, including the "combos", so, specialty, regional, family and buffet restaurants are even joining combos' promotions. This research paper presents the implementation of a system that will serve as support to elaborate combos according to the preferences of the diners using data mining techniques to find relationships between the different dishes that are offered in a restaurant. The software resulting from this research is being used by the mobile application Food Express, with which it communicates through webservices.

---

[*] Tecnológico Nacional de México, Campus Apizaco, Computer Systems Department,
Fco I Madero, Barrio de San José, 90300 Apizaco, Tlaxcala, México, rvazlean@hotmail.com,
edbonn@hotmail.com, esanlu@hotmail.com
[**] Smartsoft America BA, Calle Adolfo López Mateos, Texcacoac, 90806 Chiautempan, México,
oatriano@smartsoftamerica.com.mx, cberruecos@smartsoftamerica.com.mx

1. INTRODUCTION

The restaurant industry is a sector of great importance for economic activity, and undoubtedly, it is a factor of economic growth in many regions. The main objective in the field of food and beverages is to generate high income and have an effective management of costs. The menu is, among other factors, a key element that influences the success or failure of a restaurant.

Nowadays, blended food has been a common menu item in fast food restaurants. Food combos are a selling strategy used by restaurants to obtain higher profits and sell more products, however, most of the combos offered are formed according to the criterion of the restaurant, taking into account psychology, marketing and design to attract the attention of customers. On the other hand, on many occasions, the same customer is the one who creates his own combo based on the menu to create his own combination of meals. These last combos are the ones that take very strong interest in this research project as, if the restaurant offers combos based on the preference of the diners, you will have the security of knowing which combos are more likely to be sold and that are of the satisfaction of the diner.

The software resulting from this research work is in operation, since it is part of the Food Express application, whose objective is to order food at home, reserve or order to take away. The application is developed for the iOS and Android platforms as well as a web system (www.foodexpress.com.mx). From this application the preferences of the diners are obtained through the use of web-services to which the client has access.

The main objective of this research work is to implement a system that serves as support to assemble combos according to the preferences of the diners, which will be achieved with the historical data that will be obtained from the knowledge base that stores the food orders of the restaurants, likewise, it is intended to support the analysis of the menu and determine which are the most profitable dishes for the restaurant and the preference of the diner, what will allow to assemble the combos that could be of the diners' preference and offer them as an alternative of election. On the other hand, the system will offer to provide the diner with a list of suggested dishes that have been sold together with a dish that has been chosen by the diner.

2. LITERATURE REVIEW

This section describes some research work about association rules to classify, discover and highlight acts that occur in common within a data set and observe the relationship between them.

Some research works use the Apriori algorithm to find association rules in databases, such is the case of the work carried out by Park S. & Park Y. (2018) in which he uses the Apriori algorithm to analyze the relationship between math scores and problem solving patterns of students through the data of students' math tests by searching for association rules. On the other hand, the work of Zulfikar, Wahana, Uriawan & Lukman (2016) was carried out with the objective of helping the XMART company of Indonesia, to elaborate sales strategies. The author uses the Apriori algorithm, with values of support and confidence between the products in order to analyze the high frequency pattern and determine the association rules based on the combination of products and thus be able to show the promotions that the company can make to increase the product sales.

Other works propose making combinations of the Apriori algorithm with other algorithms to improve and optimize the results obtained. Huang, Lin & Li (2018) evaluate the use of a method called Apriori-BM applied to the conventional Apriori algorithm, which finds the association rules in the calculation process early, so it does not require repeated scanning of the database as the conventional Apriori algorithm does. In the research work carried out by Harikumar & Dilipkumar (2016) it is proposed a variant of the Apriori algorithm that uses the concept of QR decomposition to reduce the dimensions of the databases, thus reducing the complexity of the traditional Apriori algorithm. Pei (2013) proposes the application of the Apriori algorithm, improving it with the Eclat algorithm, performing operations more quickly and efficiently. In the same way, the research work of Zheng (2007) proposes the implementation of the Apriori algorithm by complementing it with the CBA-CB algorithm (Classification Based on Associations-Classifier Builder), which is applied on the rules generated by the Apriori algorithm, and thus be able to filter the most significant.

Other researchers propose other techniques for the extraction of association rules, such is the case of the work carried out by Tom & Annaraud (2017) which is mainly focused on the restaurant sector and specifically on the menu analysis. The purpose of this study is to apply fuzzy multi-criteria decision making (FMCDM) techniques to restaurant menu engineering by utilizing menu items' popularity and contribution margin. This study uses the model proposed by Kasavana and Smith where each menu item is classified into one of four segments created by a two-by-two matrix of high and low popularity, and above and below average contribution margin. Finally, Kabir, Xu, Kang & Zhao (2015) presents an evolutionary approach to find sets of frequent maximum elements of large databases by using the principles of Genetic Algorithm (GA).

3. METHODOLOGY

The development of this research work is mainly based on the implementation of the Apriori algorithm for the extraction of association rules to develop a system that allows the elaboration of combos and provide suggestions of dishes according to the preferences of the diners, serving as support to the Food Express application.

3.1. Association rules

Association rules are used to discover facts that occur in common within a given set of data. Based on the concept of strong rules Agrawal and Srikant (1994) introduced association rules to discover regularities between products in large-scale transaction data recorded by point-of-sale (POS) systems in supermarkets. This information can be used as a basis to make decisions about marketing activities. Following the definition of Agrawal and Srikant (1994), an association rule is defined as:

Let I = {i_1, i_2, ..., i_n} be a set of n binary attributes called *items*. Let D = {t_1,t_2,...,t_n} be a set of transactions called the *database*. Each transaction in **D** has a unique transaction **ID** and contains a subset of the items in **I**. A rule is defined as implication of the form **X→Y** where **X**, **Y**⊆ **I** and **X∩Y** = ∅**.** The set of items (for short *itemsets*) X and Y are called antecedent (left-hand-side or LHS) and consequent (right-hand-side or RHS) of the rule respectively.

To limit the number of rules obtained, metrics are used to measure the importance or interest of a rule, these being the following:

Support. The support **supp(X)** of an itemset **X** is defined as the proportion of transactions in the data set which contains the itemset.

$$Supp(X) = \frac{NoTransactions\_Itemset\_X}{Total\_No\_Transactions} \tag{1}$$

Given a rule "If A => B", the support of this rule is defined as the number of times or the (relative) frequency with which A and B appear together in a transaction database. Support can be defined for individual items, however, it can also be defined for the rule. A first criterion that can be imposed to limit the number of rules is that they comply with minimal support.

Confidence. The confidence of a rule is defined:

$$Conf(X \rightarrow Y) = \frac{Supp(X \cup Y)}{Supp(X)} \tag{2}$$

Given a rule "If A => B", the confidence of this rule is given by the quotient of the support of the rule and the support of the antecedent only. If the support measures frequency, confidence measures the strength of the rule. In language of probability, confidence is a strength of the rule.

Lift. The lift of a rule is defined as:

$$Lift(X \rightarrow Y) = \frac{Supp(X \cup Y)}{Supp(X) * Supp(Y)}$$ (3)

Given a rule "If A => B", the lift of this rule is given by the quotient of the support of the rule and the product of the individual supports. If the Lift = 1 or very close to 1, it indicates that the relationship is very close to having been the product of chance. If the Lift > 1, it indicates a really strong relationship (controlling for the frequency with which both occur), that is, it indicates that the relationship is much more frequent than what chance (complements) indicates. If the Lift < 1, it indicates a relatively weak relation (controlling for the frequency with which both occur), that is, that the relation appears less frequently than the chance one indicates.

3.2. Apriori algorithm

Apriori is an algorithm proposed by R. Agrawal and R. Srikant (1994) to mine sets of frequent elements for Boolean association rules. The name of the algorithm is based on the fact that the algorithm uses prior knowledge of the frequent properties of the set of elements. Apriori employs an iterative approach known as a level search, where k-sets of elements are used to explore (k + 1) – itemset. First, the set of frequent 1-itemset is found by scanning the database to accumulate the count of each element and collecting the elements that satisfy the minimum support. The resulting set is denoted by **L1**. Next, **L1** is used to find **L2**, which is used to find **L3**, and so on, until more frequent **k-itemsets** are found. The finding of each **Lk** requires a complete analysis of the database.

To improve the efficiency of the generation of sets of frequent elements at level, an important property called Apriori property is used to reduce the search space. The Apriori property is based on the fact that if a set of elements does not satisfy the minimum support threshold (min_supp), then it is not frequent, that is, P(I) < min_supp. If an element A is added to the set of elements, then the resulting element (that is, I∩A) cannot happen more often than I. Therefore, I∩A is also not frequent, that is, P(I∩A) < min_sup.

This property belongs to a special category of properties called antimono-tonicity in the sense that, if a set cannot pass a test, all its supersets will also fail the same test. This is called antimonotonicity because the property is monotonous in the context of the failure of a test (Han, Kamber & Pei, 2012). Figure 1 shows the Apriori algorithm.

```
Ck: Candidate item set of size k
         Lk: Frequent item set of size k
    L1 = {frequent items};
For (k = 1; Lk! = ϕ; k++) do begin
Ck+1 =  candidates generated from Lk;
For each transaction t in database do
         Increment the count of all candidates in Ck+1
         Those are contained in t
Lk+1 = candidates in Ck+1 with min_support
End
Return Uk Lk;
```

Fig. 1. Apriori Algorithm

An application example of the algorithm is shown below. Let be the item set:

TID	Items
1	A, B
2	A, B, C, D
3	A, B, D, F
4	A, C, D, E
5	B, C, D, F
6	A, B, D

Where, the value as minimum support will be 0.5, that is:

$$min\_supp = 0.5$$

L1 is calculated (where L1 are the elements that satisfy the minimum support and those that do not satisfy it are eliminated):

L1:

Item	Frecuency	Support
A	5	5/6=0.83
B	5	5/6=0.83
C	3	3/6=0.5
D	5	5/6=0.83
E	1	1/6=0.16
F	2	2/6=0.33
L1		

Resulting set
A
B
C
D
L2

With the **L2** list, the cartesian product is calculated, thus obtaining the possible combinations that can there be of the products (**C2**), that is, **C2 = L2XL2**, and subsequently, the minimum support for **L2** is calculated, resulting in **L3**.

C2 = L2XL2

L2		L2		C2		C2	Count	Support		Resulting set
A	X	A	=	{A,B}	→	{A,B}	4	4/6=0.66	→	{A,B}
B		B		{A,C}		{A,C}	2	2/6=0.33		{A,D}
C		C		{A,D}		{A,D}	4	4/6=0.66		{B,D}
D		D		{B,C}		{B,C}	2	2/6=0.33		{C,D}
				{B,D}		{B,D}	4	4/6=0.66		L3
				{C,D}		{C,D}	3	3/6=0.5		
						C2 Support				

With **L3**, the Cartesian product is calculated, thus obtaining the possible combinations that can there be of the products (**C3**), that is, **C3 = L3XL3**, and subsequently, the minimum support for **C3** is calculated, resulting in **L4**.
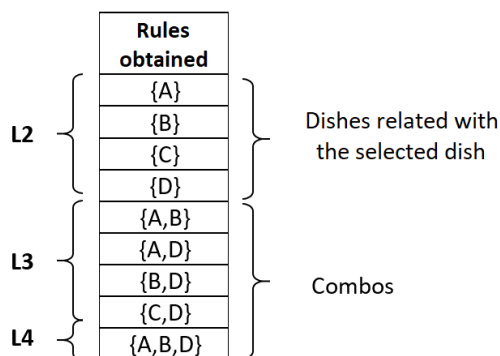
C3=L3XL3

L3		L3		C2		C2	Count	Support		Resulting set
{A,B}	X	{A,B}	=	{A,B,D}	→	{A,B,D}	3	4/6=0.66	→	{A,B,D}
{A,D}		{A,D}		{A,B,C,D}		{A,B,C,D}	1	1/6=0.16		L4
{B,D}		{B,D}		{A,D,C}		{A,D,C}	2	2/6=0.33		
{C,D}		{C,D}		{B,C,D}		{B,C,D}	2	2/6=0.33		
						C3 Support				

Because **L4** only has one itemset, it is no longer possible to make more combinations, so the resulting rules are derived from **L2**, **L3** and **L4**, being as follows:

	Rules obtained	
L2	{A}	Dishes related with the selected dish
	{B}	
	{C}	
	{D}	
L3	{A,B}	Combos
	{A,D}	
	{B,D}	
	{C,D}	
L4	{A,B,D}	

4. IMPLEMENTATION OF APRIORI ALGORITHM

The programming of the classes and methods necessary for the implementation of the Apriori algorithm was done in the Java programming language through the IDE editor Netbeans. Likewise, it was necessary to create a database for the functionality of the system with the MySQL relational database manager with the help of the phpMyAdmin tool, since it allows us to manage the database in a more dynamic and simple way.

The database consists of three tables, the first corresponds to the table that stores the keys of the restaurants that are registered, the second stores the keys of the dishes offered by each restaurant, and the third table stores the orders registered by the restaurants. Figure 2 shows the tables of the database and their relationships.

Fig. 2. Database of the system and its relations

The algorithm returns two possible values: one, **the list of suggested combos of the selected restaurant**, or two, **the list of dishes that are sold together with a dish that the diner has selected**.

4.1. Steps to get the combos and frequent dishes

To calculate the list of combos and frequent dishes, the programmed Apriori algorithm executes the following main steps:
1. You get from the table **dishes** from the Restaurants database the list of dishes offered by the restaurant and it is added to the *Candidates Set*.
2. The transactions made by the restaurant are obtained from the table **orders** of the Restaurant database.
3. The database of the transactions is scanned and the support of each subset of elements k of the *Candidate Set* is calculated.
4. The value of the support obtained from each subset of candidate elements k is compared with the *minimum support* value.
5. If the support value of each subset of candidate elements k is greater than or equal to the *minimum support* value, the subset of candidate elements k is added to the *Auxiliary Candidate Set*, that is, elements that do not comply with the *minimum support* are eliminated.

6. The elements of the *Auxiliary Candidate Set* are added to the *Association Rules Set* together with their corresponding support value.
7. The Cartesian product of the *Auxiliary Candidate Set* is calculated.
8. The values of the *Candidate Set* are replaced by the values obtained by calculating the Cartesian product.
9. If the number of elements of the *Candidate Set* is greater than 1, then return to step 3, otherwise, the value of the *Candidate Set* is added to the *Association Rules Set* with its support value.
10. The *Association Rules Set* is ordered according to the support value of each subset of candidate elements k.

In case of requiring the list of combos suggested by the Apriori algorithm, subsets that contain more than one element will be taken from the *Association Rules Set*.

In case of requiring the *list of dishes purchased together with a dish selected by the diner*, the database of transactions will consist of the **extraction of the transactions that contain the dish that the diner selected**, that is, there will not be taken into account the totality of the orders or transactions registered by the restaurant. The procedure will begin in step 3. Finally, from the *Association Rules Set* those subsets that contain only one element will be taken.

4.2. Functioning tests of the Apriori algorithm

To verify the proper functioning of the Apriori programmed algorithm, tests were carried out on data obtained from surveys to diners about the dishes that are their preference from the menu of a restaurant in the region. The number of dishes offered by the restaurant is 108, while the transactions or orders obtained from the survey were 191.

The minimum support value was reduced until the algorithm showed association rules, since the greater the support, the fewer the number of rules obtained, leaving as a minimum support value of 0.1. The association rules obtained are **12** and are shown in figure 3 and the resulting combos are shown in figure 4.

```
INFORMACIÓN:   Rule 1:  {support= 0.35, rule=PL-A }
INFORMACIÓN:   Rule 2:  {support= 0.25, rule=PL-XXA }
INFORMACIÓN:   Rule 3:  {support= 0.21, rule=PL-K }
INFORMACIÓN:   Rule 4:  {support= 0.19, rule=PL-A PL-XXA }
INFORMACIÓN:   Rule 5:  {support= 0.17, rule=PL-A PL-K }
INFORMACIÓN:   Rule 6:  {support= 0.15, rule=PL-BT }
INFORMACIÓN:   Rule 7:  {support= 0.14, rule=PL-K PL-XXA }
INFORMACIÓN:   Rule 8:  {support= 0.14, rule=PL-A PL-K PL-XXA }
INFORMACIÓN:   Rule 9:  {support= 0.12, rule=PL-D }
INFORMACIÓN:   Rule 10: {support= 0.12, rule=PL-G }
INFORMACIÓN:   Rule 11: {support= 0.11, rule=PL-T }
INFORMACIÓN:   Rule 12: {support= 0.10, rule=PL-M }
```

Fig. 3. Association rules obtained with a minimum support threshold value of 0.1

81

```
Combo 1:                           ▫▶  INFORMACIÓN: --------------------
    PL-A (Order of fruit)          ▷▷  INFORMACIÓN: Recommended Combos:
    PL-XXA (Orange Juice)          ▣   INFORMACIÓN: --------------------
Combo 2:                           ⟳   INFORMACIÓN: Combo: 1
    PL-A (Order of fruit)              INFORMACIÓN: [PL-A]
    PL-K (Eggs with ham)               INFORMACIÓN: [PL-XXA]
Combo 3:                               INFORMACIÓN: Combo: 2
    PL-K (Eggs with ham)               INFORMACIÓN: [PL-A]
    PL-XXA (Orange Juice)              INFORMACIÓN: [PL-K]
Combo 4:                               INFORMACIÓN: Combo: 3
    PL-A (Order of fruit)              INFORMACIÓN: [PL-K]
    PL-K (Eggs with ham)               INFORMACIÓN: [PL-XXA]
    PL-XXA (Orange Juice)              INFORMACIÓN: Combo: 4
                                       INFORMACIÓN: [PL-A]
                                       INFORMACIÓN: [PL-K]
                                       INFORMACIÓN: [PL-XXA]
```

Fig. 4. Combos obtained with a minimum support threshold value of 0.1

On the other hand, if you want to show the diner a list of dishes that have been purchased together with a dish you have selected, the results could be the following:

Assuming that the dish selected by the diner is the one with the key PL-B (fruit with yogurt and granola), the association rules obtained with the minimum threshold value are 15 and are shown in figure 5.

The dishes purchased frequently with the dish PL-B (fruit with yogurt and granola) are PL-G (Buñuelo), PL-XXA (Orange Juice) and PL-BT (Chocolate Milk) as shown in figure 6.

```
▫▶  INFORMACIÓN:     Rule 1:   {support= 1.00, rule=PL-B }
▷▷  INFORMACIÓN:     Rule 2:   {support= 0.67, rule=PL-G }
▣   INFORMACIÓN:     Rule 3:   {support= 0.67, rule=PL-XXA }
⟳   INFORMACIÓN:     Rule 4:   {support= 0.67, rule=PL-BT }
    INFORMACIÓN:     Rule 5:   {support= 0.67, rule=PL-B PL-G }
    INFORMACIÓN:     Rule 6:   {support= 0.67, rule=PL-B PL-XXA }
    INFORMACIÓN:     Rule 7:   {support= 0.67, rule=PL-B PL-BT }
    INFORMACIÓN:     Rule 8:   {support= 0.67, rule=PL-G PL-XXA }
    INFORMACIÓN:     Rule 9:   {support= 0.67, rule=PL-G PL-BT }
    INFORMACIÓN:     Rule 10:  {support= 0.67, rule=PL-XXA PL-BT }
    INFORMACIÓN:     Rule 11:  {support= 0.67, rule=PL-B PL-G PL-XXA }
    INFORMACIÓN:     Rule 12:  {support= 0.67, rule=PL-B PL-G PL-BT }
    INFORMACIÓN:     Rule 13:  {support= 0.67, rule=PL-B PL-G PL-XXA PL-BT }
    INFORMACIÓN:     Rule 14:  {support= 0.67, rule=PL-B PL-XXA PL-BT }
    INFORMACIÓN:     Rule 15:  {support= 0.67, rule=PL-G PL-XXA PL-BT }
```

Fig. 5. Association rules obtained with the minimum support threshold value of 0.1 for the PL-B dish

```
INFORMACION: --------------------
INFORMACIÓN: Dishes related with the dish selected by the user
INFORMACIÓN: --------------------
INFORMACIÓN: Item: 1
INFORMACIÓN: [PL-G]
INFORMACIÓN: Item: 2
INFORMACIÓN: [PL-XXA]
INFORMACIÓN: Item: 3
INFORMACIÓN: [PL-BT]
```

Fig. 6. Frequent dishes acquired with the PL-B dish with minimum support of 0.1

5. INTEGRATION OF THE COMBOS GENERATION MODULE TO THE FOOD EXPRESS APPLICATION

Because the system will be used by the Food Express application, WebService technology will be used, since they are distributed applications that are based on a series of protocols and standards for exchanging information, allowing applications to communicate with each other, regardless of language or platform in which they are developed. To implement the web service, the following resources were used: Java Development Kit JDK, NetBeans IDE 8.2 and the Application Server GlassFish Server.

To allow communication between the digital platform and the Apriori algorithm module, the communication protocol for the transfer of REST information and the response format for JSON data exchange was used.

The Food Express application will make requests to the WebService through HTTP requests and the Web Service will return as an answer either an array in JSON format that contains the list of the combos that result from the execution of the algorithm or, in another case, an array in JSON format that stores the list of dishes that have been purchased together with the dish that the diner has selected. The above is illustrated in Figure 7, which shows the communication between the client and the web service (Module).
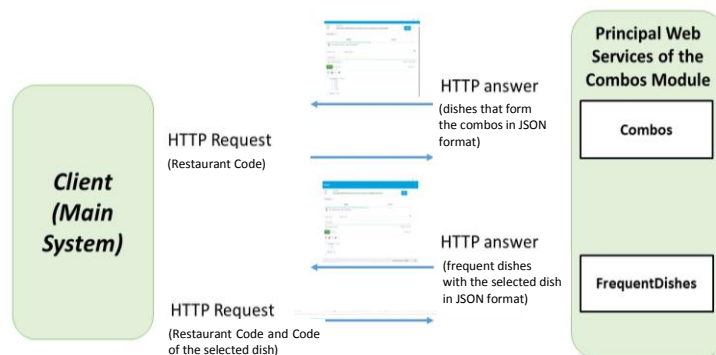

Fig. 7. Communication between the client and the web service

To carry out the communication between the webservice and the combos' module, the necessary methods and operations for communication, administration and configuration of the services offered by the Apriori module were created. Figure 8 shows a diagram with the services created and offered by the WebService, as well as the methods each service has communication with.
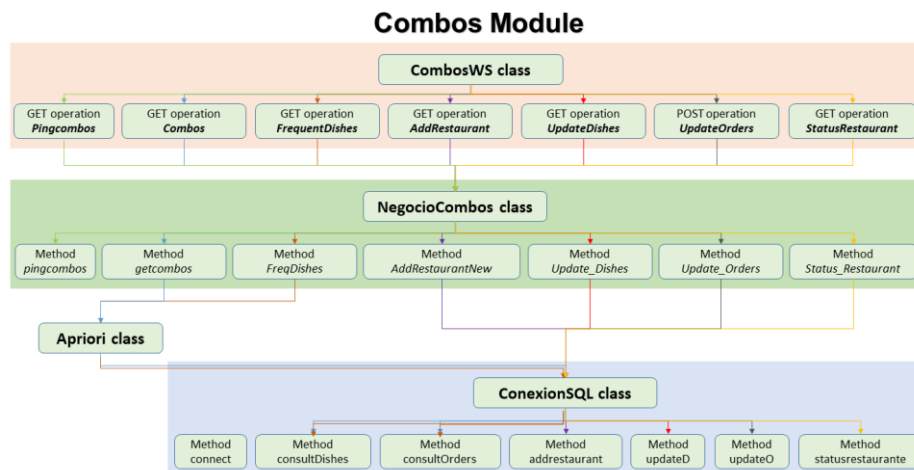

Fig. 8. Diagram of Web Service Combos classes

Table 1 specifies the necessary values for its correct operation, as well as the services implemented.

Tab. 1. WebServices for the administration, configuration and communication of the module

WS' name: *Pingcombos*	
Operation type: GET	**Input values (URL):** WebServiceCombos/service/moduloService/pingcombos
Descripción: Check the connection to the server by returning the message "In connection with the server".	
WS' name: *AddRestaurant*	
Operation type: GET	**Input values (URL):** WebServiceCombos/service/moduleService/AddRestaurant/{IdRestaurant}
Descripción: Insert a restaurant in the database of the module. It receives as parameter the restaurant ID and returns as a response the message "Restaurant added".	
WS' name: *UpdateDishes*	
Operation type: GET	**Input values (URL):** WebServiceCombos/service/moduleService/updateDishes/{IdRestaurant}/{KeyDish}
Descripción: Insert a dish into the module database. It receives as parameter the key of the restaurant and the key of the dish. Returns the message "Dish added".	

84

Tab. 2. WebServices – cont.

WS' name: *UpdateOrders*	
Operation type: POST	**Input values (URL):** WebServiceCombos/service/moduleService/updateOrders
Descripción: Add a command to the module database. It receives as parameter an object in JSON format with the Id of the restaurant, the Id of the command and the Id of the dish. Returns the message "Successful element added".	
WS' name: *StatusRestaurant*	
Operation type GET	**Input values (URL):** WebServiceCombos/service/moduleService/StatusRestaurant/{IdRestaurant}/{Status}
Descripción: Change the status of a restaurant in the database of the module, receiving as parameter 1 (activated) or 0 (Disabled). Returns the message "Element on / Element deactivated successfully".	
WS' name: *FrequentDishes*	
Operation type: GET	**Input values (URL):** WebServiceCombos/service/moduleService/frequentDishes/{IdRestaurant}/{selected Dishes}/{dishesLimit}
Descripción: Returns the dishes that are frequently purchased with a selected dish, limiting them to the number of elements requested. It receives as parameters the Id of the restaurant, the Key of the selected dish and the limit number of dishes related to be displayed.	
WS' name: *Combos*	
Operation type: GET	**Input values (URL):** WebServiceCombos/service/moduleService/combos/{IdRestaurant}/{CombosLimit}
Descripción: Returns the combos suggested by the algorithm, limiting them to the number of combos requested. It receives as parameters the Id of the restaurant and the limit number of combos to be displayed.	

5.1. Acquisition of the clients' preferences from the mobile application

The implementation of the module of combos leads to the interaction with the own processes of the mobile Food Express application to which it is integrated. This interaction is represented in cases of usage of each service belonging to the module. Figure 9 shows the case of the use of Combos service and figure 10 shows the case of usage of frequent meals service.
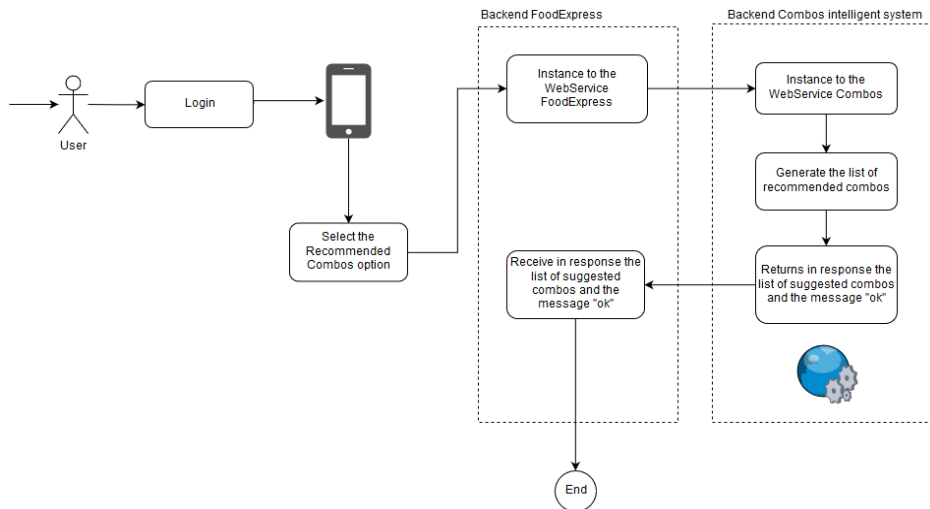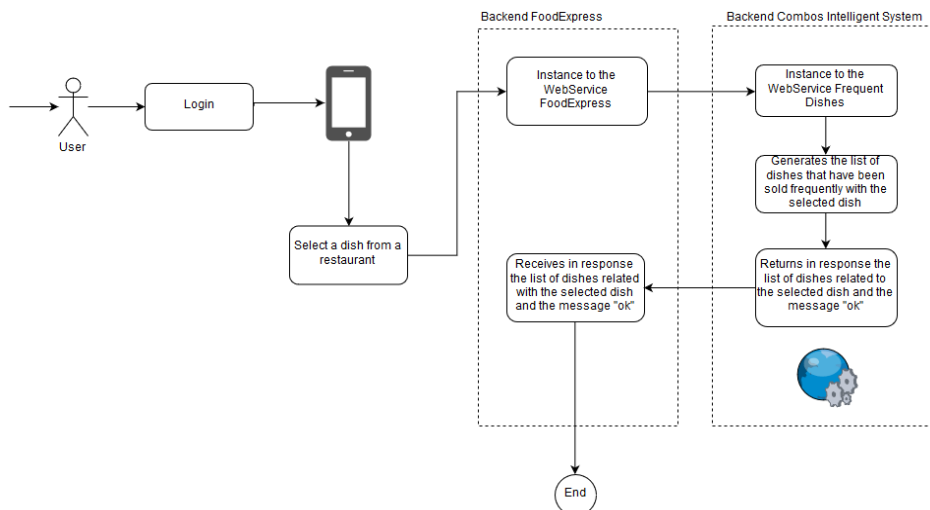
Fig. 9. Use Case of the Combos Service

Fig. 10. Use Case of the Frequent Dishes Service

5.2. Monitoring of outputs

To realize the tests with the webservice and observe the outputs, the Advanced REST Client application provided by Google was downloaded to create and test the personalized HTTP requests. Advanced REST Client is considered as the only REST client that makes the connection directly in the socket that gives total control over the connection and the request/response headers. With the application, it was possible to corroborate that the service works correctly with the specified values, so it was integrated as a web service for the Food Express application.

6. CONCLUSIONS

In this document, information is presented on the development of the Module for the Generation of Combos in restaurants for the Food Express application. Comparing several investigated methodologies, it was concluded that the Apriori Algorithm is perfectly suited to solve the problems posed.

When programming the Apriori algorithm, tests were performed to optimize the classes and methods to maintain a certain level of code quality in the program. To carry out the tests, the SonarQube application was used to audit the code of the application during programming. SonarQube is an open source tool for the analysis and improvement of the code quality of a program.

On the other hand, considering the importance of performing stress tests on the developed software, it became necessary to undertake the task of performing the tests with the Apache JMeter ™ application, which is an open source software designed to load the functional behavior of Test and measure performance.

The processes for the implementation of the combos module were evaluated in a timely manner, carrying out the necessary tests to monitor that the module carried out the operative processes efficiently and effectively, and thus, detect any problems that may arise for its proper functioning.

The functioning tests of the Apriori algorithm show that the algorithm yields the frequent items within a transaction base, which guarantees that the combos suggested by the algorithm are obtained based on the preferences of the diners, acting in the same way to obtain the elements that are frequently acquired with a selected element. Likewise, it was observed that the Apriori algorithm programmed in the Java language has problems when executing high dimension data.

The module will run as a web service, which will be accessed by the Food Express application through HTTP requests made by the client. All the processes are executed in the server and this will be responsible for returning the results to the device that requests it, so that the Apriori algorithm is carried out in the form of a black box, thus achieving its independence.

This project is a contribution that allows to generate a change in the way in which diners interact with restaurants, at the same time, it is a resource available for the restaurant industry, which will be the one that dictates through the use and operation of this system the viability of them.

REFERENCES

Agrawal, R. & Srikant, R. (1994). Fast Algorithms for Mining Association Rules in Large Databases. In *Proceedings of the 20th International Conference on Very Large Data Bases* (pp. 487-499). Santiago de Chile.

Han, J., Kamber, M., & Pei, J. (2012). Data Mining Concepts and Techniques. Third Edition. Waltham, USA: Elsevier.

Harikumar, S., & Dilipkumar, D. U. (2016). Apriori algorithm for association rule mining in high dimensional datas. In *2016 International Conference on Data Science and Engineering (ICDSE)* (pp. 1–6). Cochin. doi:10.1109/ICDSE.2016.7823952.

Huang, Y., Lin, Q., & Li, Y. (2018). Apriori-BM Algorithm for Mining Association Rules based on Bit Set Matrix. In *2018 2nd IEEE Advanced Information Management, Communicates, Electronic and Automation Control Conference (IMCEC)* (pp. 2580–2584). Xi'an. doi:10.1109/IMCEC.2018.8469367

Kabir, M. M. J., Xu, S., Kang B. H., & Zhao, Z. (2015). Comparative Analysis of Genetic Based Approach and Apriori Algorithm for Mining Maximal Frequent Item Sets. In *2015 IEEE Congress on Evolutionary Computation (CEC)* (pp. 39–45). Sendai. doi:10.1109/CEC.2015.7256872.

Park, S., & Park, Y. (2018). Analysis of Association Between Students' Mathematics Test Results Using Association Rule Mining. In *2018 International Conference on Platform Technology and Service (PlatCon)* (pp. 1–6). Jeju. doi:10.1109/PlatCon.2018.8472756

Pei, S. (2013). Application of data mining technology in the tourism product's marketing CRM. In *2013 2nd International Symposium on Instrumentation and Measurement, Sensor Network and Automation (IMSNA)* (pp.400–403). Toronto, ON. doi:10.1109/IMSNA.2013.6743300.

Tom, M., & Annaraud, K. (2017). A fuzzy multi-criteria decision making model for menu engineering. In *2017 IEEE International Conference on Fuzzy Systems (FUZZ-IEEE)* (pp. 1–6). Naples. doi:10.1109/FUZZ-IEEE.2017.8015612.

Zheng, X. Z. (2007). Building Personalized Recommendation System in E-Commerce using Association Rule-Based Mining and Classification. In *2007 International Conference on Machine Learning and Cybernetics* (pp. 4113–4118). Hong Kong. doi:10.1109/ICMLC.2007.4370866.

Zulfikar, W. B., Wahana, A., Uriawan, W., & Lukman, N. (2016). Implementation of association rules with apriori algorithm for increasing the quality of promotion. In *2016 4th International Conference on Cyber and IT Service Management* (pp. 1–5). Bandung. doi:10.1109/CITSM.2016.7577586.

Katarzyna GOSPODAREK [0000-0002-4338-4249]*

DETERMINATION OF RELATIVE LENGTHS OF BONE SEGMENTS OF THE DOMESTIC CAT'S LIMBS BASED ON THE DIGITAL IMAGE ANALYSIS

Abstract

This paper is an introduction to the issues related to obtaining information on the metric dimensions of selected bone segments of a domestic cat based on the analysis of digital images. The main objective is to acquire this data using only image processing methods. Particular emphasis was placed on obtaining data on the proportions between specific bones within the limbs. This data will be used in the process of creating a project of a four-legged walking robot whose structure will be inspired by solutions characteristic of the analyzed species.

1. INTRODUCTION

Obtaining information on the dimensions of individual bones, e. g. those belonging to the limbs of a specific animal species is a very time-consuming process. In most cases, access to appropriate X-rays or prepared bones is required. This issue becomes even more complex for species whose skeletons are less frequently analyzed, as exemplified by cats. In the case of the felids (Felis catus) family, it is extremely difficult to obtain accurate information on the dimensions of individual bone segments. The bone examination is usually associated with key segments such as femur or tibia, and it is difficult to find data for other segments (Schmidt, 2005; Udrescu & Van Neer, 2004). There is also a lack of data concerning the proportions, e. g. between individual limb bones. The majority of researchers who

---

* Czestochowa University of Technology, Faculty of Mechanical Engineering and Computer Science, Institute of Computer and Information Science, 73 Dabrowskiego Str., 42-200 Czestochowa, Poland, kgospodarek@icis.pcz.pl

analyze the anatomy of cats focus their analysis on the measurement of angles obtained in the joints, both mechanical and anatomic, and on the extraction of natural tilt angles of selected bone segments (Brown, Bertocci & Cheffer, 2018; Day & Jayne, 2007; Fonseca, Lobo-Jr & Santana, 2017; Pike & Alexander 2002).

Measurements relating to the determination of the ratio between individual bones within a cat's limbs are often omitted. Although they may provide a lot of useful information, among others on the subject of changes in the anatomical structure of the species. This may be caused by a limited number of available research materials. In the case of domestic cats, the appropriately reconstructed skeletons are extremely rare. On the other hand, their X-rays are most often taken for the purpose of bone tissue traumatology. This causes that they only cover the area of an injury. In most cases, it is a single bone or joint (Coulson & Lewis, 2002; Zwierucho & Strokowska, 2018).

There are small databases that can provide information about the metric dimensions of individual bones, but there is no information about their interrelationships within the entire skeleton. There are few papers on this subject matter. However, they highlight the problem related to the large variation in metric dimensions in the group of domestic cats. An example can be the work (O'Connor, 2007), in which a part of individuals belonging to this group was characterized by dimensions of limb bones similar to wild animals like wildcats (Felis silvestris), which are characterized by significant elongation.

The use of image processing and analysis methods in order to obtain approximate dimensions of individual bone segments for a specific species allows using materials from generally available databases in research. In this case, the dimensions can be determined on the basis of a variety of video materials or digital photos. This allows obtaining approximate data on the anatomical structure of animals, without the need for direct physical contact with the animal or its skeleton. The use of image processing in the discussed process has a significant influence on the acceleration of its course.

2. MATERIALS AND METHODS

The aim of the study was to determine the total length of limbs and the anatomical, relative mean lengths of selected bone segments of a domestic cat based on the analysis of digital images. The first database of analyzed images contained 20 digital photos representing skeletons of a selected species. Most of them were photographs of real skeletons which are exhibits in a museum or scientific centers (Fig. 1) and illustrations from anatomical atlases (Fig. 2).
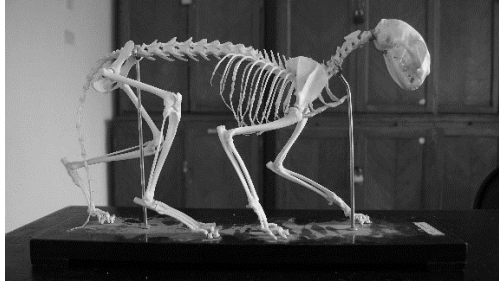
Fig. 1. Cat (Felis catus) skeleton from the collection of Moscow State University Department of Biology [source: https://meta.wikimedia.org]
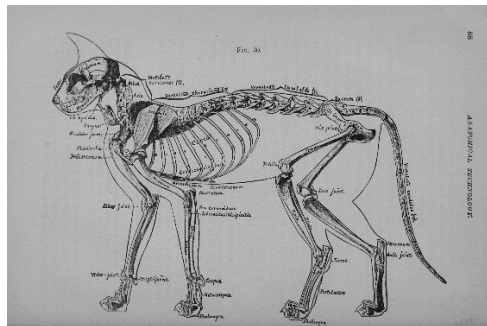

Fig. 2. Felis catus – image from the book [source: https://meta.wikimedia.org]

Each of the images under analysis was published under licenses enabling their use during the research, including CC0 type licenses – the so-called public domain transfer. The second base consisted of 20 frames isolated from various video materials containing the registered cat's gait in the sagittal plane (Fig. 3).

During the research, approximate dimensions of selected bone segments were obtained for each of the tested individuals. The following bones were analyzed: humerus, ulna/radius, metacarpals, femur, tibia/fibula, metatarsal, carpals, and phalanges (Fig.4). The total limb lengths have been calculated as the sum of the length of the respective segments, separately for the fore and hind limbs. Relative distances were calculated by dividing the specified anatomical length by the total length of the relevant limb and expressed as a percentage. During the tests, anatomically characteristic distances were also determined, for example, a two-dimensional distance between the shoulder and the hip joint

The anatomical lengths of individual bones were determined on the basis of the two-dimensional analysis of appropriately selected digital images. The measurements were carried out using Kinovea software. It is a free, powerful tool for analyzing digital images and video materials using a wide variety of measurement functions. It is mainly used for sports analyses, but due to its characteristics, it could also be used to carry out the aforementioned anatomical measurements.
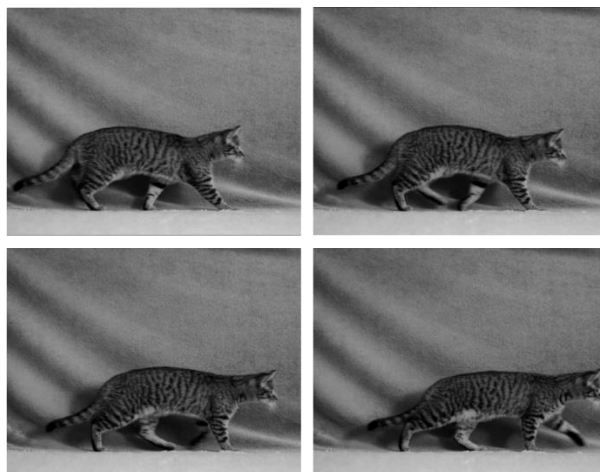
Fig. 3. Selected frames of the video sequence illustrating the cat's walk recorded in the sagittal plane

Fig. 4. Specimen of eyra cat skeleton on display at the Museum of Veterinary Anatomy, FMVZ USP (1 – humerus, 2 – ulna, 3 – metacarpals, 4 – carpals, 5 – femur, 6 – tibia, 7 – metatarsal, 8 – phalanges)

3. DESCRIPTION OF THE RESEARCH PROCESS

The research was carried out separately for two specially prepared test bases. As the first, the images containing representations of the skeleton of a domestic cat were analyzed. The second group that was analyzed were images containing representations of real individuals.
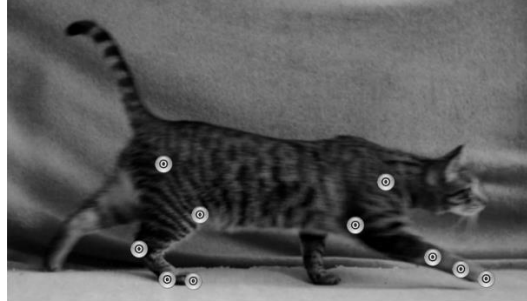
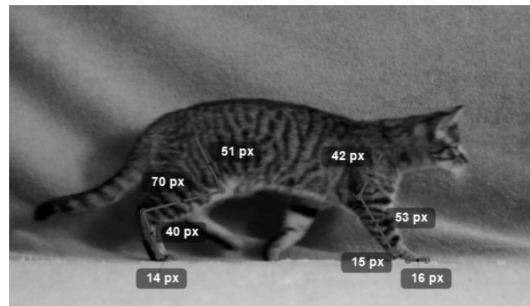**Fig. 5. Frame with marked characteristic key points**

Fig. 6. Frame with absolute lengths of segments expressed in pixels

The analysis of each database consisted of several stages. Initially, for each individual, and more precisely for his representation in the form of a digital image, characteristic key points were marked. They symbolize selected anatomical points such as joints or bony process (Fig. 5). Then the absolute lengths of individual segments expressed in pixels were determined (Fig. 6). The next step was to determine the total length of the limbs, divided into hind and fore. These data were then used as reference values in calculating the relative lengths of the analyzed bones and selected anatomical distances. These data were then used as reference values in calculating the relative lengths of the analyzed bones and selected anatomical distances. In order to obtain the most reliable results, each of the analyzed images was measured five times and the output results were based on the arithmetic mean.

The final stage of the study was to determine the mean relative lengths of each bone segments of the limbs for each of the bases separately. The sample means were determined on the basis of the formula:

$$\mu_x = \frac{\sum_{i=1}^{n} x_i}{n}, \tag{1}$$

where: μ_x – mean,
x_i – observed values,
n – number of sample.

93

For each determined length, the value of the standard deviation and the standard mean error (s. e. m.) were calculated:

$$s = \sqrt{\frac{\sum_{i=1}^{n}(x_i - \mu_x)^2}{n-1}},$$ (2)

where: s – standard deviation,
x_i – observed values,
n – number of sample,
μ_x – sample mean.

$$SE_{\mu_x} = \frac{s}{\sqrt{n}},$$ (3)

where: $SE_{\mu x}$ – standard error of the mean,
s – standard deviation,
n – number of samples.

4. RESULTS

The data obtained during the tests allowed to determine approximate lengths of specific bone segments in relation to the total length of the limbs. The results are presented in the tables below. The first (Tab. 1) contains the results obtained for a group of images containing skeleton representations. The second one contains the results obtained for a group of images containing representations of real individuals. The proportions are in accordance with the available literature data of the domestic cat's anatomy. Which allows that these results may be considered as a characteristic reference point for the analysis of the anatomical structure of the species concerned. The species characteristics obtained in the study, e. g. that the tibia is usually slightly longer than the femur, were confirmed in the analysis of research carried out in a given subject area. The same conclusions appear in the works of researchers analyzing animal skeletons directly (Fonseca et al., 2017; Petrov, 1992) and in the works related to the analysis of materials containing their recorded gait (Day & Jayne, 2007). In both cases, the differences in relative bone lengths obtained did not exceed 5%, while in terms of determining the proportion between individual bones, compliance at level 86. 33% was obtained. In only one case, discrepancies were found in the analyses. It was a relation between humerus and ulna bones.

Tab. 1. Proportional lengths of individual limb segments – results obtained for a group of images containing skeleton representations (values are means ± s. e. m.)

Hind-limb Segment	Relative Length (% Hind-limb Length)
Femur	32,90 ± 0,41
Tibia	36,43 ± 0,43
Metatarsals	20,09 ± 0,52
Phalanges	10,59 ± 0,42
Fore-limb Segment	**Relative Length (% Fore-limb Length)**
Humerus	35,75 ± 0,41
Ulna	40,84 ± 0,71
Metacarpals	12,66 ± 0,40
Carpals	10,75 ± 0,40

Tab. 2. Proportional lengths of individual limb segments – results obtained for a group of images containing representations of real individuals (values are means ± s. e. m.)

Hind-limb Segment	Relative Length (% Hind-limb Length)
Femur	30,03 ± 0,55
Tibia	36,03 ± 0,65
Metatarsals	22,68 ± 1,03
Phalanges	11,27 ± 0,44
Fore-limb Segment	**Relative Length (% Fore-limb Length)**
Humerus	34,46 ± 0,73
Ulna	42,10 ± 0,70
Metacarpals	11,59 ± 0,51
Carpals	11,85 ± 0,59

The proportions between individual limb bones determined during the analysis of digital images are consistent with the characteristics of the examined species. In all cases, the total length of the hind-limb was longer than that of the fore-limb. The tibia was usually slightly longer than the femur. The same applies to the ulna and humerus bones.

When comparing the results for both test bases, it can be seen that they are quite consistent. Differences generally do not exceed three percentage points. Although the measurements carried out for images containing pictures of living individuals were burdened with difficulties related to the necessity of partial prediction of the position of key joints. The highest correlation between the measurements for two bases was obtained in the case of tibia and humerus bone. However, the lowest correlation of measurements was obtained in the case of the femur bone.

3. CONCLUSIONS

The results obtained as part of the research were fully obtained using non-invasive measurement techniques. Determined relative lengths of individual limb bones of the analyzed species mostly coincide with the available literature data. The differences appearing in the results are mostly derived from the high intra-species diversity in cats

In order to obtain higher accuracy of results, it would be necessary to conduct the research process separately for many subgroups of individuals, with the division of gender or origin. However, it should be taken into account that even the work of researchers dealing with the subject of one subgroup of felids, characterized by a significant similarity (e.g. wildcats) show high variability of the obtained results even in the case of direct measurements (Day & Jayne, 2007; Petrov, 1992). This means that most bone length measurements in a particular species group usually give results in the form of averaged, approximate values.

The results of the study show that it is possible to measure the approximate lengths of selected bone segments in animals using procedures exclusively related to image processing and analysis. The proposed method is one of the non-invasive measurement techniques. It allows obtaining a large amount of data on species characteristics without the necessity of direct contact with the analyzed individual. This information can be extracted from the materials that are available in public databases.

The proposed methodology of collecting data on the relative length of limbs of a given species broadens the possibilities related to the analysis of skeletal anatomy. It constitutes a significant contribution to this research area, due to a very limited number of observations and related works (Day & Jayne, 2007; Fonseca et al., 2017; Petrov, 1992). The approach presented in the paper can be used in particular for the design of robots designed on the anatomical structure of specific animals. This is a promising solution because the metric features are already successfully used in the construction of humanoid robots.

REFERENCES

Brown, N., Bertocci, G. E., & Cheffer, K. A. (2018). A three dimensional multiplane kinematic model for bilateral hind limb gait analysis in cats. *PLoS One, 13*(8), 0197837. doi:10.1371/ journal.pone.0197837

Coulson, A., & Lewis, N. (2002). *An Atlas of Interpretative Radiographic Anatomy of the Dog and Cat.* UK: Blackwell Science.

Day, L. M., & Jayne, B. C. (2007). Interspecific scaling of the morphology and posture of the limbs during the locomotion of cats (Felidae). *The Journal of Experimental Biology*, *210*, 642–654. doi:10.1242/jeb.02703

Fonseca, R. L., Lobo-Jr, A. R., & Santana, M. I. S. (2017). Measurements of femoral angles, femur length, and hip width in cat radiographs. *Arquivo Brasileiro de Medicina Veterinária e Zootecnia*, *69*, 1513-1520. doi:10.1590/1678-4162-9583

O'Connor, T. P. (2007). Wild or Domestic? Biometric Variation in the Cat Felis silvestris Schreber. *International Journal of Osteoarchaeology*, *17*, 581-595. doi:10.1002/oa.913

Petrov, I. (1992). Metric characteristics and sexual dimorphism of the postcranial skeleton of wild cat Felis silvestris in Bulgaria. *Acta Theriologica*, *37*(4), 397–401.

Pike, A. V. L., & Alexander, R. M. (2002). The relationship between limb-segment proportions and joint kinematics for the hind limbs of quadrupedal mammals. *Journal of Zoology*, *258*, 427–433. doi:10.1017/S0952836902001577

Schmidt, M. (2005). Hind Limb Proportions and Kinematics: Are Small Primates Different From Other Small Mammals?. *The Journal of experimental biology*, *208*, 3367–83. doi:10.1242/jeb.01781

Udrescu, M., & Van Neer, W. (2004). Looking for human therapeutic intervention in the healing of fractures. In: R. Thomas, M. Fabis, J. Davies, I. Mainland & M. Richards (Eds.), *Diet and health in past animal populations: current research and future directions pages* (pp. 24–33). Oxford, UK: Oxbow Books.

Zwierucho, M., & Strokowska, N. (2018). Najczęstsze urazy kości oraz narządów wewnętrznych spowodowane wypadkami komunikacyjnymi – diagnostyka obrazowa oraz leczenie chirurgiczne. *Weterynaria w praktyce*, *6*, 38–50.